

ARTICLE

# Poor quality V $\beta$ recombination signal sequences stochastically enforce TCR $\beta$ allelic exclusion

Glendon S. Wu<sup>1,2</sup>, Katherine S. Yang-lott<sup>2</sup>, Morgann A. Klink<sup>2</sup>, Katharina E. Hayer<sup>2</sup>, Kyutae D. Lee<sup>2</sup>, and Craig H. Bassing<sup>1,2</sup>

**The monoallelic expression of antigen receptor (AgR) genes, called allelic exclusion, is fundamental for highly specific immune responses to pathogens. This cardinal feature of adaptive immunity is achieved by the assembly of a functional AgR gene on one allele, with subsequent feedback inhibition of V(D)J recombination on the other allele. A range of epigenetic mechanisms have been implicated in sequential recombination of AgR alleles; however, we now demonstrate that a genetic mechanism controls this process for *Tcrb*. Replacement of V(D)J recombinase targets at two different mouse V $\beta$  gene segments with a higher quality target elevates V $\beta$  rearrangement frequency before feedback inhibition, dramatically increasing the frequency of T cells with TCR $\beta$  chains derived from both *Tcrb* alleles. Thus, TCR $\beta$  allelic exclusion is enforced genetically by the low quality of V $\beta$  recombinase targets that stochastically restrict the production of two functional rearrangements before feedback inhibition silences one allele.**

## Introduction

Monoallelic expression is an essential process that limits the dosage of numerous genes. Important examples include genetic imprinting and X-chromosome inactivation, as well as the tissue-specific allelic exclusion of olfactory neuron receptors and lymphocyte antigen receptors (AgR). While genetic imprinting and X-inactivation are vital for normal development and physiology, monoallelic expression of olfactory and AgR is fundamental for highly specific recognition and responses to diverse odors or pathogens. To date, mechanisms enforcing monoallelic gene expression programs have been shown to involve epigenetic-based transcriptional activation of an expressed allele and silencing of the nonexpressed allele (Khamlichi and Feil, 2018). Lymphocyte AgR allelic exclusion requires an additional level of regulation due to the obligate assembly of AgR genes by variable (diversity) joining (V(D)J) recombination. The germline TCR and Ig AgR loci are comprised of noncontiguous variable (V), joining (J), and in some instances diversity (D) gene segments. In developing T and B lymphocytes, the RAG1/RAG2 endonuclease cleaves at recombination signal sequences (RSSs) flanking these segments to assemble V(D)J exons, which encode the antigen-binding variable regions of Ig and TCR proteins (Bassing et al., 2002; Schatz and Swanson, 2011). Due to imprecise repair of RAG DNA double-strand breaks (DSBs), only one-third of V(D)J rearrangements occur in-frame to create functional genes. In the absence of other

regulatory mechanisms, the frequent assembly of out-of-frame rearrangements and the requirement for AgR protein expression to drive T and B cell development dictate that biallelic expression of any TCR or Ig gene should occur in 20% of lymphocytes (Brady et al., 2010; Mostoslavsky et al., 2004). However, most AgR loci exhibit stringent allelic exclusion, presumably the result of mechanisms that enforce sequential assembly of their two respective alleles (Brady et al., 2010; Levin-Klein and Bergman, 2014; Mostoslavsky et al., 2004; Outters et al., 2015; Vettermann and Schlissel, 2010). At least for *Igk* loci, RAG DSBs on one allele signal down-regulation of RAG expression and inhibition of V $\kappa$  recombination on the other allele (Steinel et al., 2013). In addition, expression of a given AgR protein after the in-frame assembly of one allele often signals permanent feedback inhibition of V rearrangements on the opposing allele, at least in part via epigenetic changes that halt V recombination (Brady et al., 2010; Levin-Klein and Bergman, 2014; Mostoslavsky et al., 2004; Outters et al., 2015; Vettermann and Schlissel, 2010).

The mechanisms by which immature lymphocytes ensure sequential assembly of the two TCR $\beta$ , IgH, or Ig $\kappa$  alleles before feedback inhibition remain unknown (Brady et al., 2010; Levin-Klein and Bergman, 2014; Mostoslavsky et al., 2004; Outters et al., 2015; Vettermann and Schlissel, 2010). Indeed, there is considerable disagreement about whether these mechanisms are deterministic or stochastic (Brady et al., 2010; Levin-Klein and

<sup>1</sup>Immunology Graduate Group, Perelman School of Medicine, University of Pennsylvania, Philadelphia, PA; <sup>2</sup>Department of Pathology and Laboratory Medicine, Children's Hospital of Philadelphia, Perelman School of Medicine, University of Pennsylvania, Philadelphia, PA.

Correspondence to Craig H. Bassing: [bassing@email.chop.edu](mailto:bassing@email.chop.edu).

© 2020 Wu et al. This article is distributed under the terms of an Attribution–Noncommercial–Share Alike–No Mirror Sites license for the first six months after the publication date (see <http://www.rupress.org/terms/>). After six months it is available under a Creative Commons License (Attribution–Noncommercial–Share Alike 4.0 International license, as described at <https://creativecommons.org/licenses/by-nc-sa/4.0/>).

Bergman, 2014; Mostoslavsky et al., 2004; Outters et al., 2015; Vettermann and Schlissel, 2010). Deterministic models invoke that each cell first targets only one allele for V segment recombination, with activation of the second allele only if the first is assembled out-of-frame. In contrast, stochastic models posit that both alleles can be activated within a similar time frame, but inefficient recombination of V segments renders it unlikely that a given cell will complete assembly of two alleles before feedback inhibition is engaged. Prevailing models of sequential AgR allele activation invoke epigenetic-based mechanisms, which are known to modulate many aspects of transcription, chromatin accessibility, and chromosome topology (Brady et al., 2010; Shih and Krangel, 2013). Consequently, the field has focused on identifying epigenetic phenomena that correlate with monoallelic recombination of V gene segments at *Tcrb*, *Igh*, and *Igk* loci. In this regard, the two alleles for each of these loci asynchronously replicate in lymphocytes (Mostoslavsky et al., 2001). For *Igk*, this process initiates in lymphoid progenitors, is clonally maintained, and correlates with preferential recombination of the early replicating allele (Farago et al., 2012), suggesting a deterministic mechanism for monoallelic recombination that is associated with DNA replication. For *Tcrb*, *Igh*, and *Igk*, others have shown that one of their respective alleles often resides at transcriptionally repressive nuclear structures (Chan et al., 2013; Chen et al., 2018; Hewitt et al., 2009; Schlimgen et al., 2008; Skok et al., 2007). This finding has led to models whereby differential positioning of alleles, via deterministic or stochastic mechanisms, governs asynchronous initiation of V recombination (Chan et al., 2013; Chen et al., 2018; Hewitt et al., 2009; Schlimgen et al., 2008; Skok et al., 2007). Critically, although these epigenetic mechanisms might govern the assembly of a functional AgR gene on one allele before epigenetic-based silencing of further V rearrangement on the opposing allele by feedback inhibition, causality has not been established for any.

A component of this assembly process that has largely been overlooked with regard to allelic exclusion is the recombination substrate itself, the RSSs that flank each gene segment. RSSs consist of a semi-conserved heptamer and nonamer separated by a nonconserved 12 or 23 nucleotide spacer (Schatz and Swanson, 2011). The binding of an RSS forces RAG to adopt an asymmetric conformation that permits functional synapsis and cleavage with a different-length RSS (Kim et al., 2018; Ru et al., 2015). This RSS-determined restriction of RAG activity along with the types of RSSs flanking V, D, and J segments limits V(D)J rearrangements to those with a potential for generating functional AgR genes (Bassing et al., 2000; Jung et al., 2003). The recombination quality, or strength, of an RSS is determined by its interactions with a partner RSS, RAG, and HMGB1 proteins that bend the DNA substrate (Banerjee and Schatz, 2014; Drejer-Teel et al., 2007; Jung et al., 2003). Natural variations in RSS sequences can influence recombination patterns (Akira et al., 1987; Connor et al., 1995; Gauss and Lieber, 1992; Hesse et al., 1989; Larijani et al., 1999; Livak et al., 2000; Nadel et al., 1998; Oлару et al., 2004; Ramsden and Wu, 1991; VanDyk et al., 1996; Wei and Lieber, 1993). This is most profound for *Tcrb*, where V $\beta$ s are flanked by poor 23-RSSs, D $\beta$ s by strong 5' 12-RSSs and 3' 23-RSSs, and J $\beta$ s by poor 12-RSSs (Banerjee and Schatz, 2014; Drejer-Teel et al., 2007; Jung et al., 2003; Tillman et al., 2003;

Wu et al., 2003). The low qualities of V $\beta$  RSSs prevent their recombination with J $\beta$  RSSs and thereby focus V $\beta$  rearrangements to DJ $\beta$  complexes (Banerjee and Schatz, 2014; Drejer-Teel et al., 2007; Jung et al., 2003; Tillman et al., 2003; Wu et al., 2003). At least for the atypical V $\beta$  segment (V31) that resides near D $\beta$ -J $\beta$  segments and rearranges by inversion, V $\beta$  RSS identity rather than V $\beta$  transcription and chromatin accessibility is a major factor that limits its recombination frequency (Wu et al., 2003; Yang-Iott et al., 2010).

Here, we demonstrate that low V $\beta$  RSS quality provides a major underlying genetic, rather than epigenetic, mechanism to enforce TCR $\beta$  allelic exclusion by minimizing initiation of V $\beta$  recombination on both alleles. We show that replacement of two different V $\beta$  RSSs with a better-quality D $\beta$  RSS in mice increases V $\beta$  rearrangement frequency before TCR $\beta$ -signaled feedback inhibition, thereby elevating the fraction of T cells that expresses TCR $\beta$  protein from both alleles. In addition, we show that each V $\beta$  RSS replacement allele competes with its homologous *Tcrb* allele for recombination, indicating that both alleles can be active for V $\beta$  recombination within the same time frame. We conclude that TCR $\beta$  allelic exclusion is enforced genetically by the poor qualities of V $\beta$  RSSs, which stochastically limit the assembly of functional *Tcrb* genes on each allele before feedback inhibition can epigenetically silence V $\beta$  recombination.

## Results

### Generation of V $\beta$ RSS replacement mice with grossly normal $\alpha\beta$ T cell development

The *Tcrb* locus contains 23 functional V $\beta$ s positioned 250–735 kb upstream of the D $\beta$ 1-J $\beta$ 1-C $\beta$ 1 and D $\beta$ 2-J $\beta$ 2-C $\beta$ 2 clusters, each of which has one D $\beta$  and six functional J $\beta$ s (Fig. 1 A). *Tcrb* has another V $\beta$  (*Trbv31*, hereafter called V31) located 10 kb downstream of C $\beta$ 2 and in the opposite transcriptional orientation from all other *Tcrb* coding sequences (Malissen et al., 1986). To determine potential roles of low-quality V $\beta$  RSSs in governing TCR $\beta$  allelic exclusion, we made C57BL/6 mice carrying germline replacement of the V31 and/or *Trbv2* (V2) RSS with the stronger 3' D $\beta$ 1 RSS, referred to as the V2<sup>R</sup> or V31<sup>R</sup> modifications (Fig. 1, A and B; and Fig. S1). We created and studied mice with each distinct modification on one (V2<sup>R/+</sup>, V31<sup>R/+</sup>), both (V2<sup>R/R</sup>, V31<sup>R/R</sup>), or opposite alleles (V2<sup>R/+</sup>/V31<sup>R/+</sup>). All of these mutant mice have normal numbers and frequencies of mature  $\alpha\beta$  T cells and thymocytes at each developmental stage (Fig. 1 C and Fig. S2, A–F). In thymocytes, D $\beta$ -to-J $\beta$  rearrangement initiates at the DN1 stage and continues in DN2 and DN3 stages, while V $\beta$ -to-DJ $\beta$  recombination occurs only at the DN3 stage (Godfrey et al., 1993). To study rearrangements of V2<sup>R</sup> and V31<sup>R</sup> alleles without the influence of an opposing *Tcrb* allele, we introduced the WT, V2<sup>R</sup>, or V31<sup>R</sup> alleles opposite an allele lacking the *Tcrb* enhancer (E $\beta$ ), whose loss blocks all *Tcrb* rearrangements in cis (Bories et al., 1996; Bouvier et al., 1996). We found that V2<sup>R</sup> and V31<sup>R</sup> rearrangements initiate in DN3 cells but occur at much greater levels than V2 and V31 rearrangements (Fig. S3, A–C). Thus, replacement of the V2 or V31 RSS with the 3' D $\beta$ 1 RSS substantially increases the frequency of V2 or V31 recombination without altering normal development of  $\alpha\beta$  T cells.

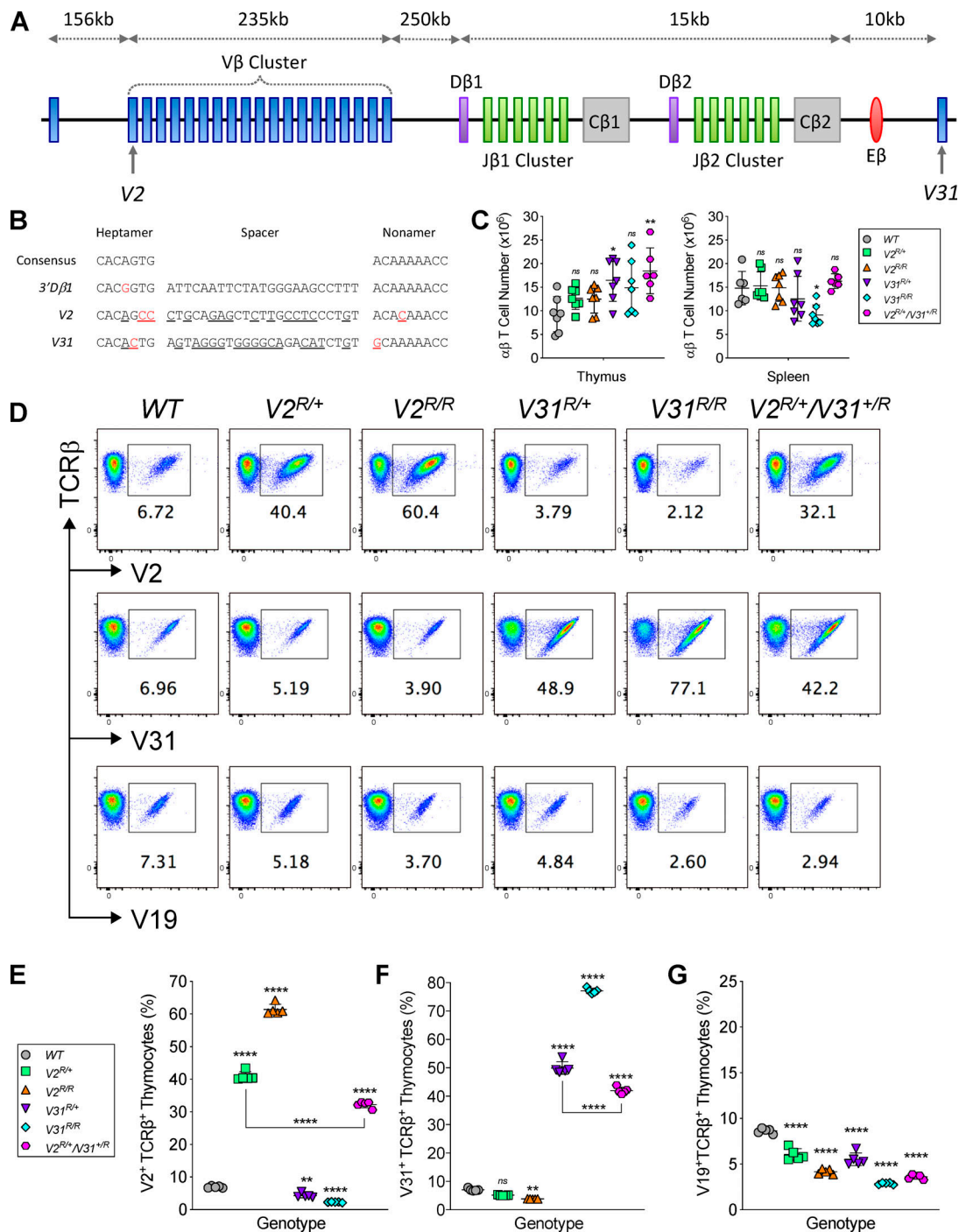


**Figure 1. Increased utilization of 3'Dβ1 RSS-replaced Vβ segments on αβ T cells.** (A) Schematic of the *Tcrb* locus and relative positions of V, D, and J segments, C exons, and the Eβ enhancer. Not drawn to scale. (B) Sequences of a consensus heptamer and nonamer and the 3'Dβ1, V2, and V31 RSSs. Differences relative to the consensus heptamer and nonamer are indicated in red. Differences of each Vβ RSS relative to the 3'Dβ1 RSS are underlined. (C) Total numbers of SP thymocytes and splenic αβ T cells ( $n \geq 6$  mice per group). (D) Representative plots of SP thymocytes expressing V2<sup>+</sup>, V31<sup>+</sup>, or V19<sup>+</sup> TCRβ chains. (E–G) Quantification of V2<sup>+</sup> (E), V31<sup>+</sup> (F), or V19<sup>+</sup> (G) SP thymocytes; refer to legend in D.  $n = 5$  mice per group, one-way ANOVA followed by Dunnett's post-tests comparing each RSS mutant to WT (B) or Tukey's post-tests for multiple comparisons (E–G). ns, not significant; \*,  $P < 0.05$ ; \*\*,  $P < 0.01$ ; \*\*\*\*,  $P < 0.0001$ . All quantification plots show mean  $\pm$  SD. Data in C and E–G are compiled from five experiments.

**RSS-replaced Vβs outcompete unmodified segments in the TCR repertoire**

In WT C57BL/6 mice, Vβ representation is similar in αβ TCR repertoires of CD4<sup>+</sup> or CD8<sup>+</sup> single positive (SP) T cells and

mirrors relative levels of Vβ rearrangement in DN3 cells (Wilson et al., 2001). We performed flow cytometry on SP thymocytes and naive splenic αβ T cells to determine whether RSS substitutions impact recombination and resultant usage of

individual V $\beta$ s within the  $\alpha\beta$  TCR repertoire. We used a C $\beta$ -specific antibody along with antibodies that bind a single V $\beta$  (V2, *Trbv4* [V4], *Trbv19* [V19], or V31) or a family of V $\beta$ s (*Trbv12.1* and *Trbv12.2* [V12] or *Trbv13.1*, *Trbv13.2*, and *Trbv13.3* [V13]). In WT mice, 7.0% of SP cells express V2<sup>+</sup> or V31<sup>+</sup> TCR $\beta$  chains on their surface (Fig. 1, D–F). For mice with each V $\beta$  RSS replacement on one or both alleles, we detected a 6–11-fold elevated representation of the modified V $\beta$  on SP thymocytes (Fig. 1, D–F). Specifically, 40.9% of V2<sup>R/+</sup> cells and 61.4% of V2<sup>R/R</sup> cells expressed V2<sup>+</sup> TCR $\beta$  chains, while 50.0% of V31<sup>R/+</sup> cells and 77.1% of V31<sup>R/R</sup> cells expressed V31<sup>+</sup> TCR $\beta$  chains (Fig. 1, D–F). As all genotypes have similar numbers of SP cells (Fig. 1 C), the increased usage of each modified V $\beta$  must be at the expense of other V $\beta$  segments. Indeed, there were fewer V31<sup>+</sup> cells in V2<sup>R/+</sup> and V2<sup>R/R</sup> mice relative to WT mice (5.1% and 3.8%, versus 7.0%; Fig. 1, D–F) and fewer V2<sup>+</sup> cells in V31<sup>R/+</sup> and V31<sup>R/R</sup> mice compared with WT mice (4.3% and 2.3%, versus 7.0%; Fig. 1, D–F). Additionally, the percentage of cells expressing V4<sup>+</sup>, V12<sup>+</sup>, V13<sup>+</sup>, or V19<sup>+</sup> TCR $\beta$  protein was reduced in V2<sup>R/+</sup> and V31<sup>R/+</sup> mice, and more so in V2<sup>R/R</sup> and V31<sup>R/R</sup> mice (Fig. 1, D and G; Fig. S4, A–E; and data not shown). The altered repertoires of V $\beta$  RSS replacement mice show that the 3'D $\beta$ 1 RSS empowers V2 and V31 to outcompete normal V $\beta$  segments for recombination and resultant usage in the  $\alpha\beta$  TCR repertoire.

We noted that each homozygous RSS-replaced genotype used its modified V $\beta$  segment ~1.5 times more than their heterozygous counterpart (Fig. S4 F). This less-than-additive effect implies that both *Tcrb* alleles compete with each other for rearrangement and usage in the  $\alpha\beta$  TCR repertoire. The repertoires of V2<sup>R/+</sup>, V31<sup>R/+</sup>, and V2<sup>R/+</sup>/V31<sup>R/+</sup> cells yield further evidence for allelic competition, as each modified V $\beta$  is less represented in V2<sup>R/+</sup>/V31<sup>R/+</sup> mice relative to V2<sup>R/+</sup> or V31<sup>R/+</sup> mice (Fig. 1, D–F; and Fig. S4, A–C). These differences imply that the overall V $\beta$  recombination efficiency of each RSS-replaced allele is elevated such that it outcompetes the homologous allele. To further test this possibility, we analyzed WT/*E $\beta$ <sup>Δ</sup>*, V2<sup>R</sup>/*E $\beta$ <sup>Δ</sup>*, and V31<sup>R</sup>/*E $\beta$ <sup>Δ</sup>* mice in which the E $\beta$ -deleted (*E $\beta$ <sup>Δ</sup>*) allele cannot compete with the functional allele. The percentages of V2<sup>+</sup> and V31<sup>+</sup> SP cells each are similar between WT/*E $\beta$ <sup>Δ</sup>* and WT mice (Fig. 2, A–D). In contrast, each RSS-replaced V $\beta$  is used ~1.5 times more in V2<sup>R</sup>/*E $\beta$ <sup>Δ</sup>* or V31<sup>R</sup>/*E $\beta$ <sup>Δ</sup>* mice compared with V2<sup>R/+</sup> or V31<sup>R/+</sup> mice, respectively (Fig. 2, A–D), and the percentages of V2<sup>+</sup> and V31<sup>+</sup> cells are similar to V2<sup>R/R</sup> and V31<sup>R/R</sup> mice (compare Fig. 1, D–F, with Fig. 2, A–D). To our knowledge, the only demonstrated function of the endogenous E $\beta$  element is to drive *Tcrb* recombination. Thus, while we cannot rule out the contribution of another function of E $\beta$ , our data suggest that each RSS-replaced V $\beta$  segment outcompetes for rearrangement the other V $\beta$ s on both alleles.

### V $\beta$ RSS replacements increase biallelic assembly and expression of functional TCR $\beta$ genes

To determine potential effects of V $\beta$  RSS replacements on TCR $\beta$  allelic exclusion, we performed flow cytometry to quantify  $\alpha\beta$  T cells that stain with two different anti-V $\beta$  antibodies because of a lack of allotypic markers that identify TCR $\beta$  chains encoded by each allele. We used this approach to determine the

percentages of  $\alpha\beta$  T cells expressing two different types of TCR $\beta$  chains, first with an antibody for V2 or V31 in combination with V4, V12, V13, or V19 antibodies. For each combination, we observed that 0.05–0.21% of SP cells stained with both antibodies in WT mice (Fig. 3, A–D). We detected increased frequencies of SP cells that stained for V31 and each other V $\beta$  tested in V31<sup>R/+</sup> and V31<sup>R/R</sup> mice (Fig. 3, C and D), and likewise, for V2 and each other V $\beta$  assayed in V2<sup>R/+</sup> and V2<sup>R/R</sup> mice (Fig. 3, A and B). In WT mice, 0.09% of SP thymocytes were V2<sup>+</sup>V31<sup>+</sup>, which increased to 0.3–0.68% of cells in mice carrying V2<sup>R</sup> or V31<sup>R</sup> on one or both alleles (Fig. 3, E and F). Strikingly, the frequency of V2<sup>+</sup>V31<sup>+</sup> SP cells is increased 27-fold in V2<sup>R/+</sup>/V31<sup>R/+</sup> mice compared with WT mice (2.47% versus 0.09%, Fig. 3, E and F). The 3.5-fold greater frequency of V2<sup>+</sup>V31<sup>+</sup> cells in V2<sup>R/+</sup>/V31<sup>R/+</sup> mice compared with mixed V2<sup>R/R</sup> and V31<sup>R/R</sup> cells provides firm evidence for  $\alpha\beta$  T cells expressing both V2<sup>+</sup> and V31<sup>+</sup> TCR $\beta$  chains. The sum of double-staining cells for all V $\beta$  combinations tested indicates that the fraction of  $\alpha\beta$  T cells expressing two distinct TCR $\beta$  proteins in V2<sup>R/+</sup>/V31<sup>R/+</sup> mice is 4.5-fold greater than normal (Fig. 3 G). We note similar findings in splenic  $\alpha\beta$  T cells (Fig. S5, A–G). Collectively, these data demonstrate that replacement of a single V $\beta$  RSS with the 3'D $\beta$ 1 RSS on one or opposite alleles elevates the frequencies of  $\alpha\beta$  T cells expressing two different types of TCR $\beta$  protein.

To determine if V $\beta$  RSS replacements increase biallelic assembly of functional TCR $\beta$  genes, we created 102  $\alpha\beta$  T cell hybridomas from V2<sup>R/+</sup>/V31<sup>R/+</sup> mice and analyzed *Tcrb* rearrangements. We compared our data to a prior study of 212 WT hybridomas, where 56.6% contained a single V $\beta$  rearrangement on one allele and DJ $\beta$  rearrangement on the other allele (V(D)J/DJ; Table 1), and 43.4% contained an in-frame and an out-of-frame V $\beta$  rearrangement on opposite alleles (V(D)J/V(D)J; Table 1; Khor and Sleckman, 2005). Of our V2<sup>R/+</sup>/V31<sup>R/+</sup> hybridomas, 45.1% were V(D)J/DJ and 31.4% were V(D)J/V(D)J (Table 1). Unexpectedly, 23.5% of V2<sup>R/+</sup>/V31<sup>R/+</sup> hybridomas had two V $\beta$  rearrangements (V31 and another V $\beta$ ) on one allele, which has never been observed in WT cells (23.5% versus 0%; Table 1 and Fig. S5 H; Khor and Sleckman, 2005). We also observed V31 recombination directly to J $\beta$  segments in 23.5% of V2<sup>R/+</sup>/V31<sup>R/+</sup> hybridomas (Table 1). Such direct V $\beta$ -to-J $\beta$  rearrangements rarely occur and have only been reported in hybridomas from mice carrying replacement of the V31 RSS with the better 3'D $\beta$ 1 RSS or the J $\beta$ 1.2 RSS with the stronger 5'D $\beta$ 1 RSS (Bassing et al., 2000; Sleckman et al., 2000; Wu et al., 2003, 2007). Finally, we found that eight (7.8%) of the V2<sup>R/+</sup>/V31<sup>R/+</sup> hybridomas had recombination of both V2<sup>R</sup> and V31<sup>R</sup> (Table 1). Notably, two of these contained an in-frame V2DJ $\beta$  rearrangement on one allele and an in-frame V31DJ $\beta$  rearrangement on the other allele (Table 1 and Table 2), mirroring the 2.47% of V2<sup>+</sup>V31<sup>+</sup> cells detected by flow cytometry. While our hybridoma analysis provides unequivocal evidence that V $\beta$  RSS replacements on opposite alleles increase the overall frequency of V $\beta$  recombination, our sample size precludes concrete evidence for an elevated frequency of biallelic in-frame V $\beta$  rearrangements. However, by considering our hybridoma and flow cytometry data together, we conclude that replacement of a V $\beta$  RSS with the 3'D $\beta$ 1 RSS on opposite alleles increases the overall frequency

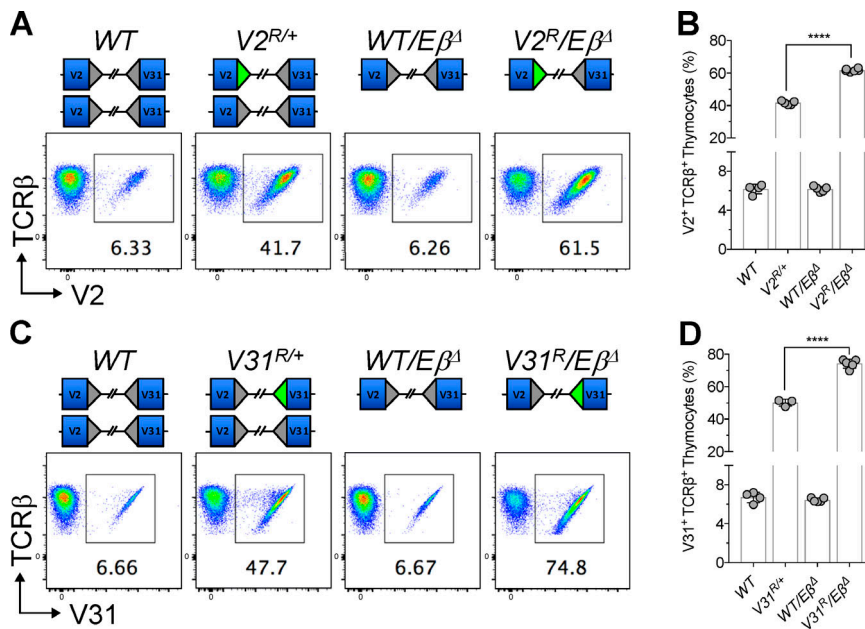


**Figure 2. Vβ RSS replacement alleles compete with normal *Tcrb* alleles for usage in the TCRβ repertoire.** (A and C) Representative plots of SP thymocytes expressing V2<sup>+</sup> (A) or V31<sup>+</sup> (C) TCRβ chains. (B and D) Quantification of V2<sup>+</sup> (B) or V31<sup>+</sup> (D) SP thymocytes (mean ± SD, n ≥ 3 mice per group, unpaired Student's t test; \*\*\*\*, P < 0.0001). Data in B and D are compiled from three experiments.

of Vβ rearrangements, leading to greater incidence of biallelic assembly and expression of functional *Tcrb* genes.

**The ability of the 3'Dβ1 RSS to elevate Vβ recombination does not require c-Fos binding**

The increased Vβ recombination and biallelic TCRβ expression in Vβ RSS replacement mice can be explained by the greater strength of the 3'Dβ1 RSS for recombining to Dβ and Jβ RSSs. However, 3'Dβ RSSs, but not Vβ RSSs, can bind the c-Fos transcription factor, which in turn can enhance 3'Dβ1 RSS recombination activity on plasmid substrates (Wang et al., 2008). Therefore, to address potential contributions of c-Fos on the ability of 3'Dβ1 RSS substitutions to increase Vβ recombination, we established mice carrying V2 or V31 RSS replacements with a two-nucleotide variant 3'Dβ1 RSS that cannot bind c-Fos (the V2<sup>F</sup> or V31<sup>F</sup> modification; Fig. 4, A and B; Wang et al., 2008). We analyzed mice with each variant Vβ RSS replacement on one or opposite alleles and observed normal αβ T cell development (data not shown). We found a 4.9-fold increase of V2<sup>+</sup> cells in V2<sup>F/+</sup> mice and a 5.4-fold increase of V31<sup>+</sup> cells in V31<sup>F/+</sup> mice (Fig. 4, C–E). In V2<sup>F/+</sup>/V31<sup>F/+</sup> mice, we found greater than normal frequencies of V2<sup>+</sup> and V31<sup>+</sup> cells, which were less than twice the levels in V2<sup>F/+</sup> or V31<sup>F/+</sup> mice, respectively (Fig. 4, C–E). Finally, we detected greater than normal frequencies of V2<sup>+</sup>V31<sup>+</sup> αβ T cells in V2<sup>F/+</sup>, V31<sup>F/+</sup>, and V2<sup>F/+</sup>/V31<sup>F/+</sup> mice (Fig. 4, F and G). Critically, these data indicate that the effects of the 3'Dβ1 RSS replacements at increasing Vβ recombination and biallelic TCRβ expression do not require c-Fos binding.

**Vβ RSS replacements increase the initiation of Vβ recombination before feedback inhibition**

The elevated incidences of biallelic TCRβ expression in Vβ RSS replacement mice could arise from increased Vβ recombination before feedback inhibition and/or continued Vβ recombination after feedback inhibition. We found V2 or V31 rearrangements are greater than normal in DN3 thymocytes of V2<sup>R</sup>/Eβ<sup>Δ</sup> and V31<sup>R</sup>/

Eβ<sup>Δ</sup> mice, respectively (Fig. S3 C). As Vβ segments recombine independent of competition and feedback inhibition from the Eβ<sup>Δ</sup> allele in these mice, these data indicate that the 3'Dβ1 RSS replacements increase Vβ recombination before feedback inhibition. To determine whether TCRβ-mediated feedback inhibition prevents V2<sup>R</sup> and V31<sup>R</sup> rearrangements, we generated and analyzed V2<sup>R/+</sup> and V31<sup>R/+</sup> mice expressing a preassembled functional TCRβ transgene (*Tcrb*<sup>Tg</sup>). Expression of the transgenic V13<sup>+</sup> TCRβ protein signals feedback inhibition of Vβ rearrangements in DN3 thymocytes (Steinel et al., 2010). However, ~3% of *Tcrb*<sup>Tg</sup> αβ T cells express TCRβ protein from VDJβ rearrangements that occur before *Tcrb*<sup>Tg</sup>-mediated feedback inhibition (Steinel et al., 2010). By flow cytometry, we found that the *Tcrb*<sup>Tg</sup> more effectively reduces usage of V2 than V31 when each is flanked by their own RSS or the 3'Dβ1 RSS (Fig. 5, A–D). To quantify V2<sup>R</sup> and V31<sup>R</sup> rearrangements, we made hybridomas from V2<sup>R/+</sup>, *Tcrb*<sup>Tg</sup>V2<sup>R/+</sup>, V31<sup>R/+</sup>, and *Tcrb*<sup>Tg</sup>V31<sup>R/+</sup> mice. We detected V2<sup>R</sup> rearrangement in 50% of V2<sup>R/+</sup> cells but not in any *Tcrb*<sup>Tg</sup>V2<sup>R/+</sup> cells (P = 2.68 × 10<sup>-5</sup>, Pearson's χ<sup>2</sup> test with Yates' correction), and V31<sup>R</sup> rearrangement in 50% of V31<sup>R/+</sup> cells and 15% of *Tcrb*<sup>Tg</sup>V31<sup>R/+</sup> cells (P = 1.63 × 10<sup>-5</sup>, Pearson's χ<sup>2</sup> test with Yates' correction; Table S1). Our previous analysis of 129 *Tcrb*<sup>Tg</sup> αβ T cell hybridomas showed that 2.3% had a V31 rearrangement and an additional 7% carried recombination of a different Vβ (Table S1 and data not shown; Steinel et al., 2010). These data demonstrate that *Tcrb*<sup>Tg</sup>-signaled feedback inhibition suppresses recombination of V2<sup>R</sup> and V31<sup>R</sup> and does so more effectively for V2<sup>R</sup>. One potential mechanism of feedback inhibition could involve blocking RAG access to 5'Dβ RSSs in double negative (DN) thymocytes (Bassing et al., 2000). In this scenario, recombination of V2<sup>R</sup> or V31<sup>R</sup> directly to Jβ segments would continue as TCRβ signals initiate DN-to-double positive (DP) thymocyte development. However, in hybridomas where V31<sup>R</sup> is the only Vβ that rearranged, V31<sup>R</sup> recombined with Jβ segments in 38% of V31<sup>R/+</sup> cells and 14% of *Tcrb*<sup>Tg</sup>V31<sup>R/+</sup> cells (Table S1), revealing that TCRβ-mediated feedback also inhibits V31<sup>R</sup>-to-Jβ

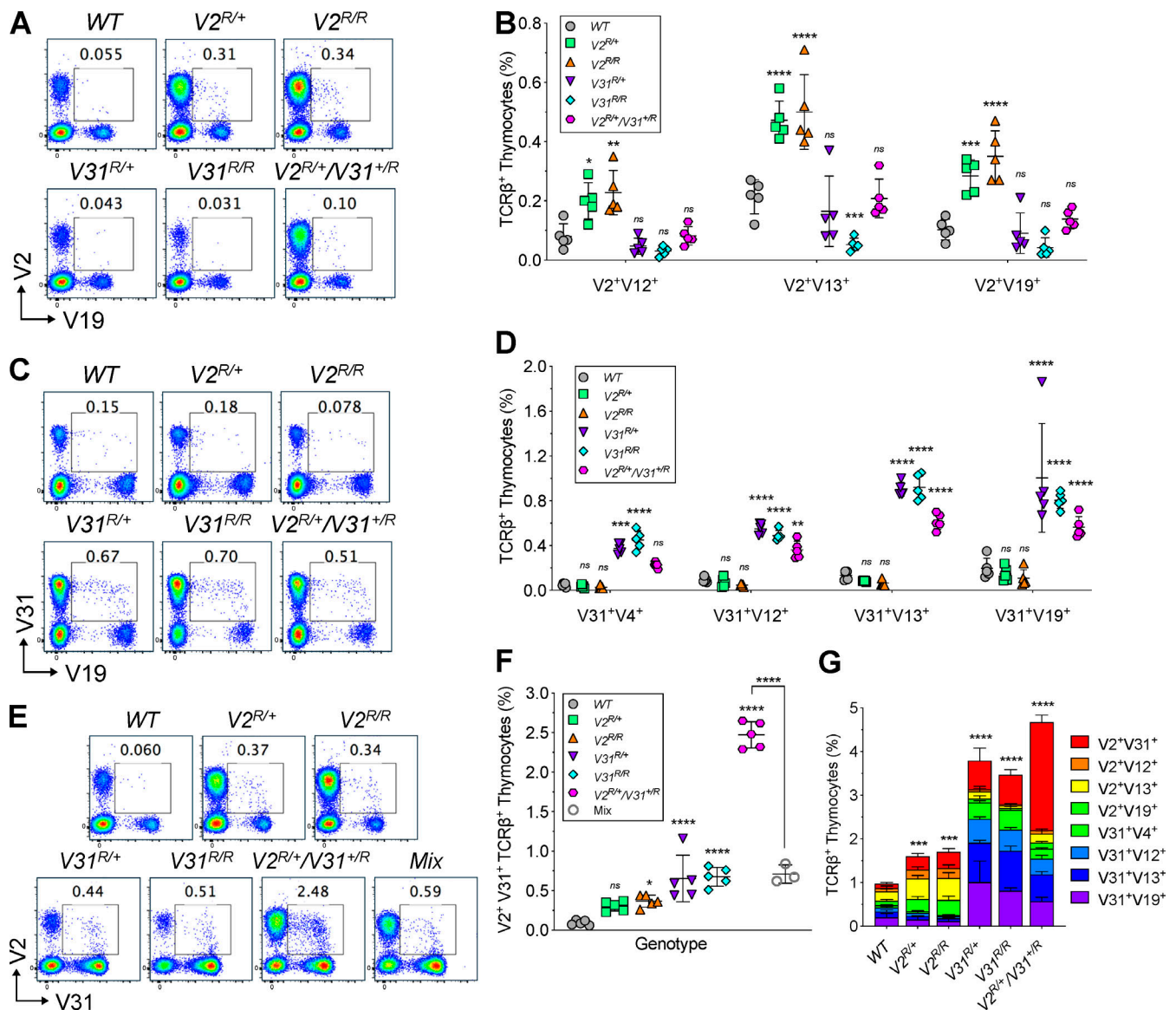


**Figure 3. 3'DB1 RSS-replaced Vβ segments increase biallelic *Tcrb* gene expression. (A, C, and E)** Representative plots of SP thymocytes expressing both V2<sup>+</sup> and V19<sup>+</sup> (A), V31<sup>+</sup> and V19<sup>+</sup> (C), or V2<sup>+</sup> and V31<sup>+</sup> (E) TCRβ chains. **(B, D, and F)** Quantification of SP thymocytes expressing the two indicated TCRβ chains. **(F)** V2<sup>R/R</sup> and V31<sup>R/R</sup> thymocytes were mixed 1:1 and analyzed. **(B and D)** *n* = 5 mice per group, two-way ANOVA followed by Dunnett's post-tests for multiple comparisons. **(F)** *n* ≥ 3 mice per group, one-way ANOVA followed by Tukey's post-tests for multiple comparisons. **(G)** Quantification of double-staining SP thymocytes for each Vβ combination tested (*n* = 5 mice per group, one-way ANOVA followed by Dunnett's post-tests comparing each RSS mutant to WT). All quantification plots show mean ± SD. ns, not significant; \*, *P* < 0.05; \*\*, *P* < 0.01; \*\*\*, *P* < 0.001; \*\*\*\*, *P* < 0.0001. Data in B, D, F, and G are compiled from five experiments.

recombination. Therefore, the increased frequency of Vβ recombination before TCRβ-mediated feedback inhibition is the mechanistic basis for the higher than normal frequencies of biallelic TCRβ expression in Vβ RSS replacement mice.

### Discussion

Our study answers a longstanding question in immunology: How do developing lymphocytes assemble only one allele of any AgR locus into a functional gene before feedback inhibition permanently halts further V recombination? In contrast to prevailing epigenetic models of sequential V rearrangements

between alleles, we demonstrate that a genetic mechanism governs monoallelic gene assembly and expression at *Tcrb* before TCRβ-signaled feedback inhibition. Specifically, improving the quality of only a single Vβ RSS on each allele increases Vβ rearrangement frequency before enforcement of feedback inhibition. The modified Vβ segments initiate recombination in DN3 thymocytes and are subject to TCRβ-signaled feedback inhibition, indicating that they still behave like Vβ segments and do not gain rearrangement properties of Dβ segments. These targeted alterations also reveal that the two *Tcrb* alleles compete with each other for Vβ recombination and, when high-efficiency Vβ-RSSs are present on both alleles, a dramatic increase in cells

Table 1. Analysis of *Tcrb* rearrangements in  $\alpha\beta$  T cell hybridomas

	Genotype				P value
	$V2^{R/+}/V31^{+/R}$		WT <sup>a</sup>		
	Number	% Total	No.	% Total	
<b>Clonal hybridomas assayed</b>	102	–	212	–	
<b>Rearrangement status</b>					
V(D)J/DJ	46	45.1	120	56.6	
V(D)J/V(D)J	32	31.4	92	43.4	
V(D)J-V(D)J/DJ	10	9.8	0	0	1.842 <sup>-10</sup>
V(D)J-V(D)J/V(D)J	14	13.7	0	0	
Monoallelic V(D)J	56	54.9	120	56.6	0.9597
Biallelic V(D)J	46	45.1	92	43.4	0.9455
1 V(D)J	46	45.1	120	56.6	0.3305
2 V(D)J	42	41.2	92	43.4	0.8995
3 V(D)J	14	13.7	0	0	1.039 <sup>-06</sup>
V2(D)J	13	12.7			
V31(D)J	58	56.9			
V31-to-DJ	33	32.4			
V31-to-J	24	23.5			
V2(D)J/ 31(D)J	8	7.8			
V2(D)J <sup>IF</sup> /V31(D)J <sup>IF</sup>	2	2.0			

P values were generated by Pearson's  $\chi^2$  test with Yates' continuity correction. IF, in-frame.

<sup>a</sup>Khor and Sleckman, 2005.

expressing TCR $\beta$  proteins from both alleles occurs. We conclude that *Tcrb* has evolved to possess poor-quality V $\beta$ -RSSs, which stochastically limit the incidence of productive V $\beta$  rearrangements on both alleles before feedback inhibition terminates their recombination in subsequent stages of thymocyte development. This stochastic genetic mechanism may cooperate with additional epigenetic processes that have been implicated in asynchronous V recombination between alleles. For example, if asynchronous *Tcrb* replication determined that the early replicating allele were preferentially activated, weak V $\beta$  RSSs might minimize V $\beta$  rearrangement on a late replicating allele before TCR $\beta$  protein from a VDJ $\beta$  rearrangement on the other allele activates feedback inhibition. Moreover, poor V $\beta$  RSSs could synergize with stochastic differential positioning of alleles at transcriptionally repressive nuclear structures to reduce the probability of V $\beta$  recombination on the second allele before TCR $\beta$ -signaled feedback inhibition from the first rearranged allele. The increased biallelic TCR $\beta$  expression of V $\beta$  RSS replacement mice involves a distinct protein from each allele and results in T cells expressing two different types of TCRs, each with their own specificity for antigen. Consequently, poor-quality V $\beta$  RSSs provide an underlying genetic mechanism for creating monospecific T cells capable of mounting highly specific adaptive immune responses to pathogens or transformed cells.

We propose the following model for TCR $\beta$  allelic exclusion. In noncycling DN3 thymocytes, both *Tcrb* alleles can become active simultaneously, but low-quality V $\beta$  RSSs stochastically

constrain V $\beta$  recombination to one allele in most cells. The resultant RAG DSBs trigger transient feedback inhibition of further V $\beta$  rearrangement, at least in part by down-regulating RAG expression (Fisher et al., 2017), providing time to test the initial rearrangement. If this rearrangement is out-of-frame, RAG re-expression after DSB repair allows V $\beta$  recombination on the second allele, or the first allele when a D $\beta$ 2J $\beta$ 2 complex is available. In the latter case, poor V $\beta$  RSSs again limit the chance for V $\beta$  recombination on both alleles. Upon an in-frame rearrangement on either allele, the encoded TCR $\beta$  protein activates cyclin D3 to move cells into S phase (Sicinska et al., 2003), where RAG2 is degraded (Lin and Desiderio, 1994). Based on data from pro-B cells (Powers et al., 2012), cyclin D3 also could repress V $\beta$  accessibility. In DN3 cells with RAG reexpressed between DSB repair and S phase entry, low-quality V $\beta$  RSSs continue to limit V $\beta$  recombination on the other allele. We propose that stochastic interactions of *Tcrb* alleles with the nuclear lamina that inhibit RAG access, V $\beta$  accessibility, and chromosome looping between V $\beta$  and D $\beta$ -J $\beta$  segments (Chan et al., 2013; Chen et al., 2018; Schlimgen et al., 2008) cooperate with poor V $\beta$  RSSs to restrain biallelic *Tcrb* gene assembly during the time DN3 cells can attempt V $\beta$  recombination. After an in-frame VDJ $\beta$  rearrangement, TCR $\beta$ -signaled transcriptional silencing of RAG expression during DN-to-DP thymocyte development prevents *Tcrb* recombination as cells rapidly proliferate and differentiate. Finally, TCR $\beta$  signals that drive differentiation of DP thymocytes activate epigenetic mechanisms that block V $\beta$  recombination

Table 2. Sequence analysis of the V2 and V31 rearrangements on opposite alleles in V2<sup>R/+</sup>/V31<sup>R/R</sup> T cell hybridomas

	Vβ	N/P	Potential Dβ	N/P	Jβ		Status	
Clone 1	V2	<u>AGCAGCCAAGA</u>	<u>TA</u>	<u>A</u>	<u>T</u>	<u>CCGGGCAG</u>	2.2	Out-of-frame
	V31	<u>GCCTGGAGTCT</u>		<b><u>AC</u></b>		<u>CCAACGAAAGA</u>	1.4	In-frame
Clone 23	V2	<u>AGCAGCCAAGA</u>	T	<u>TGG</u>		<u>GAACAG</u>	2.7	In-frame
	V31	The V31 rearrangement was not identified						
Clone 54	V2	<u>AGCAGC</u>	CAA	<u>GAC</u>		<u>AACACCGGCAG</u>	2.2	In-frame
	V31	<u>GCCTGGAGTCT</u>	A	<u>GC</u>	<u>G</u>	<u>TGAACAG</u>	2.7	Out-of-frame
Clone 55	V2	<u>AGCAGC</u>	<u>T</u>	<u>T</u>		<u>CTCCTATGAACAG</u>	2.7	In-frame
	V31	<u>GCCTGGAGTCTC</u>		<b><u>GGGACAGGGGG</u></b>	<u>GCGG</u>	<u>GAACAG</u>	2.7	In-frame
Clone 59	V2	<u>AGCAGCCAAGA</u>	<u>TC</u>	<u>GG</u>		<u>AGTCAAACACCTTG</u>	2.4	In-frame
	V31	<u>GCCT</u>		<b><u>GCC</u></b>		<u>CACCTTG</u>	2.4	Out-of-frame
Clone 62	V2	The V2(Dβ)β2 rearrangement was not cloned and sequenced						
	V31	V31-to-5'Dβ1 RSS hybrid join, deleting all subsequent Jβ1-Cβ1 and Dβ2/Jβ2-Cβ2 sequences						
Clone 90	V2	<u>AGCAGC</u>	<u>TT</u>	<u>CT</u>	C	<u>CTATGAACAG</u>	2.7	In-frame
	V31	<u>GCCTGGAGTCTC</u>	<u>CCCCT</u>	<u>CTGGGGGG</u>	<u>TGCAGAAA</u>	<u>CGCTGTATTTTGGC</u>	2.3	In-frame
Clone 105	V2	<u>AGCAGCCA</u>	<u>CCTCC</u>	<u>GGGACTGGGGC</u>	<u>TATGA</u>	<u>ACAG</u>	2.7	In-frame
	V31	V31 rearranged to the Vβ coding sequence of an out of frame V29(Dβ)β2.7 rearrangement						

Sequences are underlined every three nucleotides to orient the reading frame. Dβ nucleotides in bold are from Dβ1, italicized nucleotides are from Dβ2, and for V2 rearrangements, unformatted nucleotides could be from either.

when *Tcrα* genes assemble (Agata et al., 2007; Jackson and Krangel, 2005; Majumder et al., 2015; Skok et al., 2007). The loss of expression of the E47 transcription factor in DP thymocytes silences Vβ chromatin and recombination to maintain TCRβ allelic exclusion during *Tcrα* recombination (Agata et al., 2007). In addition to down-regulation of Vβ accessibility, diminished contacts between Vβ and Dβ-Jβ segments and additional factors that prevent RAG-mediated synapsis, cleavage, and joining of Vβ and Dβ-Jβ segments could maintain TCRβ allelic exclusion in DP thymocytes (Jackson and Krangel, 2005; Majumder et al., 2015; Skok et al., 2007). Notably, as Vβ 23-RSSs share features with V<sub>H</sub> 23-RSSs, but not other 23-RSSs (Liang et al., 2002), and Vβ and V<sub>H</sub> rearrangements are similarly activated sequentially between alleles and feedback inhibited by epigenetic mechanisms (Brady et al., 2010), all aspects of this model could apply to IgH allelic exclusion.

The field has strived to elucidate mechanisms that drive AgR locus V rearrangements across large genomic distances, with focus on factors that promote broad usage of V gene segments and enforce allelic exclusion. In vivo studies have demonstrated that V accessibility and V contact with D-J segments can influence relative V rearrangement frequency (Fuxa et al., 2004; Jain et al., 2018; Ryu et al., 2004). Computational analyses based on correlations conclude V accessibility is the predominant factor for V usage at *Tcrb* and *Igh*, while V RSS quality and contact with D-J segments each function as a binary switch to prevent or allow recombination (Bolland et al., 2016; Gopalakrishnan et al., 2013). On the contrary, our data show that V2 and V31 RSSs function far beyond reaching a minimal threshold for recombination with Dβ RSSs. The increased usage of V2<sup>R</sup> and V31<sup>R</sup> at

the expense of other Vβ segments on the same allele indicates that most, if not all, Vβs dynamically compete with each other for productive synapsis with DJβ complexes. On a normal allele, RAG protein bound to Dβ RSSs likely repeatedly captures and releases different Vβ RSSs (Wu et al., 2003), analogous to recombination between RSSs in vitro (Lovely et al., 2015). This sampling of Vβs could occur via diffusional-based synapsis of Vβ RSSs positioned in a cloud of spatial proximity (Ji et al., 2010) or by chromosomal-loop scanning-based synapsis (Jain et al., 2018). To determine RSS quality, the field typically uses an algorithm that calculates a recombination information content (RIC) score based on statistical modeling of how each nucleotide diverges from an averaged RSS (Cowell et al., 2003). The RIC scores of the RSSs that we manipulated in vivo predict the 3'Dβ1 RSS replacement would decrease V2 recombination and the variant 3'Dβ1 RSS substitution would reduce both V2 and V31 rearrangements (Fig. S5 I). The differences between predicted and empirical data could be due to several possibilities, including that the RIC algorithm does not address pairwise effects of RSSs. Regardless, the discrepancies between predictions of machine-generated associations and our in vivo data highlight the vital need to test computational-based models of V(D)J recombination. In addition to elucidating mechanisms that enforce allelic exclusion, the field has worked to identify physiological roles for monoallelic assembly and expression of *Tcrb*, *Igh*, and *Igk* genes (Brady et al., 2010). Our in vivo RSS replacement approach provides an unprecedented opportunity to test these models of biallelic assembly and expression of diverse genes, at least for *Tcrb*.

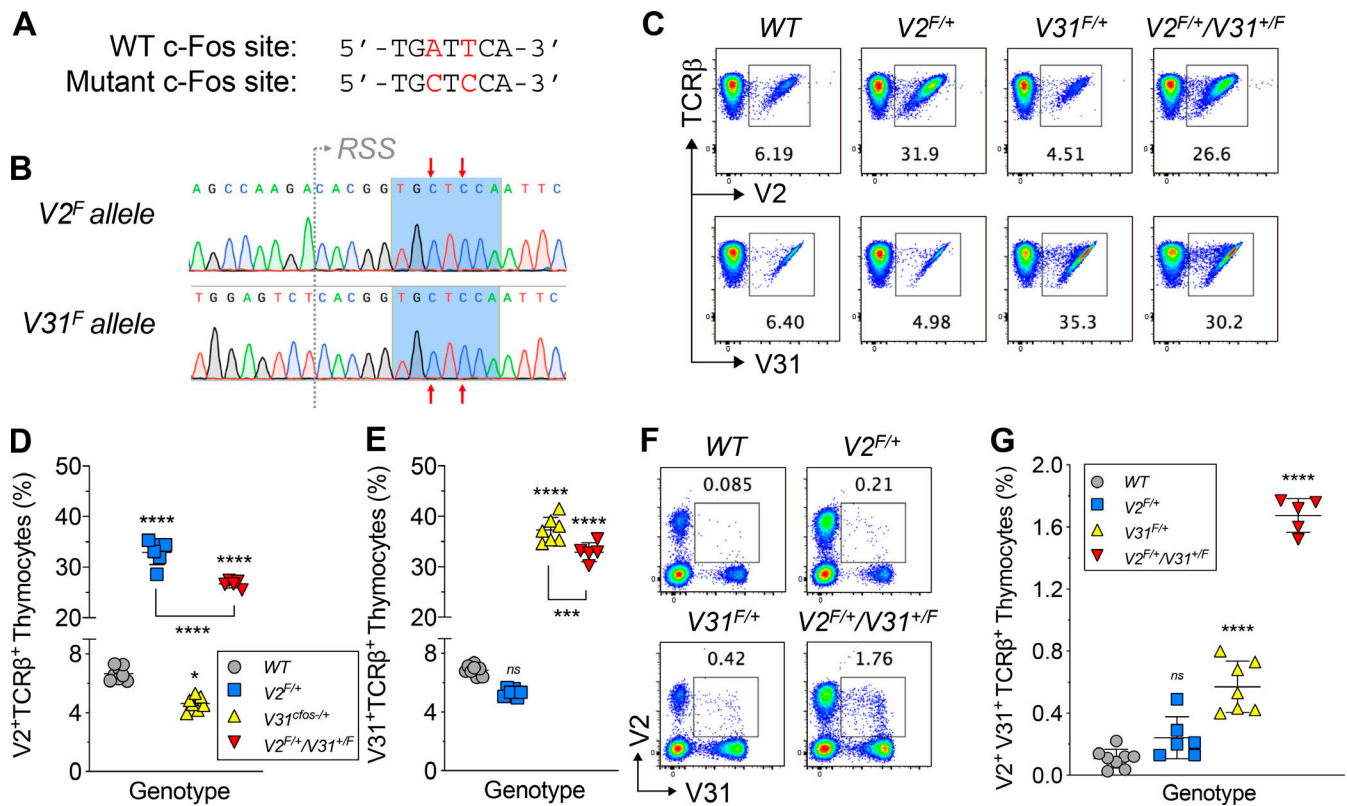


**Figure 4. 3'Dβ1 RSS substitutions increase Vβ usage and TCRβ allelic inclusion independent of c-Fos binding.** (A) Sequences of the normal and inactivated c-Fos binding site in the 3'Dβ1 RSS. The A→C and T→C mutations are indicated in red. (B) Sequence validation of the V2 or V31 RSS replacement with the variant 3'Dβ1 RSS. The inactivated c-Fos binding site is highlighted in blue and mutated nucleotides indicated by red arrows. (C) Representative plots of SP thymocytes expressing V2<sup>+</sup> or V31<sup>+</sup> TCRβ chains. (D and E) Quantification of V2<sup>+</sup> (D) or V31<sup>+</sup> (E) SP thymocytes (n ≥ 5 mice per group, one-way ANOVA followed by Tukey's post-tests for multiple comparisons). (F) Representative plots of SP thymocytes expressing both V2<sup>+</sup> and V31<sup>+</sup> TCRβ chains. (G) Quantification of SP thymocytes expressing both V2<sup>+</sup> and V31<sup>+</sup> TCRβ chains (n ≥ 5 mice per group, one-way ANOVA followed by Dunnett's post-tests comparing each RSS mutant to WT). All quantification plots show mean ± SD. ns, not significant; \*, P < 0.05; \*\*, P < 0.001; \*\*\*\*, P < 0.0001. Data in D, E, and G are compiled from three experiments.

## Materials and methods

### Mice

All experimental mice assayed in this study were 4–6 wk old, of mixed sex, and housed under specific pathogen-free conditions at the Children's Hospital of Philadelphia (CHOP). Animal husbandry, breeding, and experiments were performed in accordance with national guidelines and regulations and approved by the CHOP Institutional Animal Care and Use Committee. We used CRISPR/Cas9-mediated genomic editing in C57BL/6 zygotes to create mice carrying replacement of a V2 RSS with the normal 3'Dβ1 RSS (V2<sup>R</sup> allele) or variant 3'Dβ1 RSS (V2<sup>F</sup> allele) or a V31 RSS with the variant 3'Dβ1 RSS (V31<sup>F</sup> allele).

To replace the V2 RSS, we identified a suitable target protospacer adjacent motif 5'-AGG-3' located on the antisense strand of the V2 RSS spacer. We subcloned the 20-mer "Trbv2 gRNA target" sequence (Table S1) into the pSpCas9(BB)-2A-Puro vector and in vitro transcribed a single-stranded guide RNA using described methods (Ran et al., 2013). The CHOP Transgenic Core microinjected zygotes with a mixture of the single-stranded guide RNA (8 μM), Cas9 protein (8 μM), and a single-strand oligonucleotide (ssODNA) repair template (10 μM; Chen et al., 2016; Wang et al., 2013). To generate the V2<sup>R</sup> allele, we used the

ssODNA 5'-GGACTACTGAACTGAGTCCCCAGGCTCAGGTAGACCAGTTACATCAACAGTTTCTGGATCCACTGAGGAGGTTTTTTGTAAAGGCTTCCCATAGAATTGAATCACCGTGTCTTGGCTGCTGGCACAGAAGTATGTGGCCGAGTCATCAGGCTTTAGAGCTGTGATCTGAAGG-3' (Integrated DNA Technologies). To generate the V2<sup>F</sup> allele, we used the ssODNA 5'-GGACTACTGAACTGAGTCCCCAGGCTCAGGTAGACCAGTTACATCAACAGTTTCTGGATCCACTGAGGAGGTTTTTTGTAAAGGCTTCCCATAGAATTGGAGCACCGTGTCTTGGCTGCTGGCACAGAAGTATGTGGCCGAGTCATCAGGCTTTAGAGCTGTGATCTGAAGG-3' (Integrated DNA Technologies). For both V2<sup>R</sup> and V2<sup>F</sup> alleles, founders were identified by PCR on tail DNA using the 5'V2 and 3'Dβ1RSSRev primers and/or 3'V2 and 3'Dβ1RSS primer pairs. Each RSS replacement was then verified in homozygous mice by PCR sequencing using the 5'V2 and 3'V2 primers. For subsequent genotyping, primers 3'V2 and 3'Dβ1RSS were used to identify the V2<sup>R</sup> allele, and primers 3'V2 and V2Fos were used to identify the V2<sup>F</sup> allele (see Table S2 for a list of all primers).

To generate the V31<sup>F</sup> allele, we identified a suitable target protospacer adjacent motif 5'-AGG-3' located on the sense strand of the V31 RSS spacer. As outlined above, we used the 20-mer "Trbv31 gRNA target" (Table S1) and the ssODNA 5'-CAGGCC

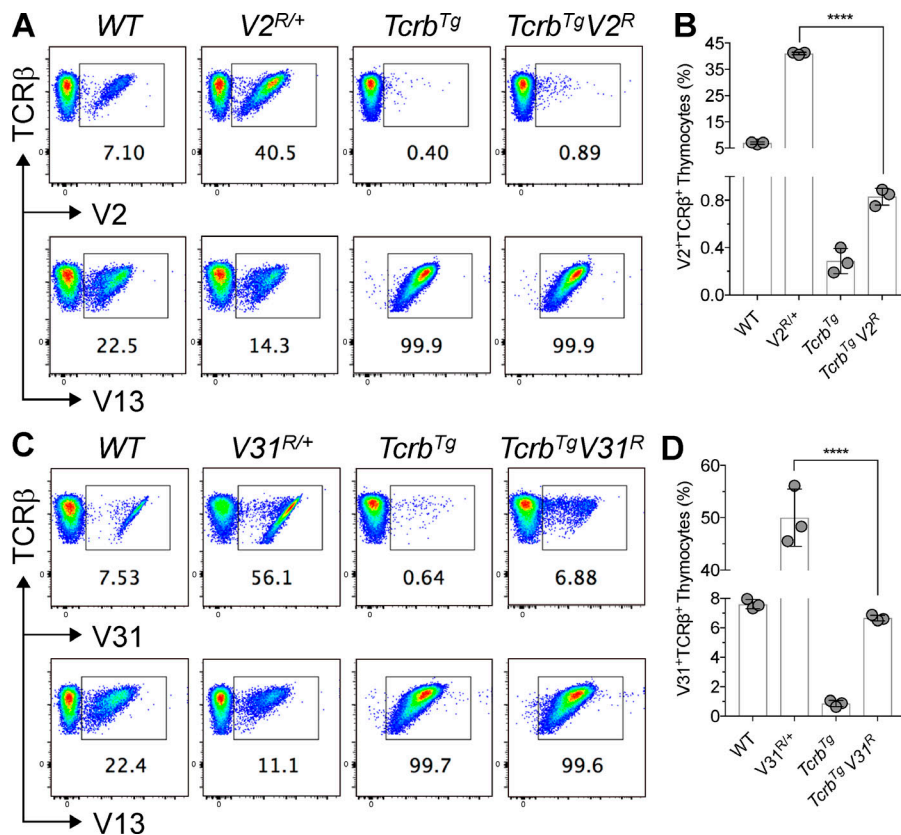


**Figure 5. 3'Dβ1 RSS substitutions increase Vβ recombination before enforcement of feedback inhibition. (A and C)** Representative plots of SP thymocytes expressing V2<sup>+</sup> (A), V31<sup>+</sup> (C), or V13<sup>+</sup> TCRβ chains. **(B and D)** Quantification of SP thymocytes expressing V2<sup>+</sup> (B) or V31<sup>+</sup> (D) TCRβ chains (*n* = 3 mice per group, unpaired Student's *t* test; \*\*\*\*, *P* < 0.0001). All quantification plots show mean ± SD. Data in B and D are compiled from three experiments.

GAAGGACGACCAATTCATCCTAAGCACGGAGAAGCTGCTTCT CAGCCACTCTGGCTTCTACCTCTGTGCCTGGAGTCTCACGGT GCTCCAATTCTATGGGAAGCCTTTACAAAAACACACCCTCT CTTTAGTCCTCCTCCCTCACTAGGAACCCTCACTAGGGATG GGTGGAGGGGTTTGCCACTGAATTT-3' (Integrated DNA Technologies). Founders were identified by PCR on tail DNA using the 5'V31 and 3'Dβ1RSSRev and/or the 3'V31 and 3'Dβ1RSS primer pairs. The RSS replacement was verified in homozygous mice by PCR-sequencing using the 5'V31 and 3'V31 primers. For subsequent genotyping, primers 3'V31 and 3'Dβ1RSS were used to identify the V31<sup>R</sup> allele and primers 3'V31 and V31Fos were used to identify the V31<sup>F</sup> allele (see Table S2 for a list of all primers).

We bred the V2<sup>R</sup>, V2<sup>F</sup>, and V31<sup>F</sup> alleles of founding mice to C57BL/6 mice for two to five generations. We then crossed heterozygous Vβ RSS replacement mice with each other, V31<sup>R/+</sup> mice (Horowitz and Bassing, 2014), Eβ<sup>Δ/Δ</sup> mice (Leduc et al., 2000), or Tcrb<sup>Tg</sup> mice (Shinkai et al., 1993), to establish experimental mice as well as WT controls. To genotype V2<sup>R/+</sup>/V31<sup>R/+</sup> mice, we used the 3'V2 and 3'Dβ1RSS primers to identify the V2<sup>R</sup> allele and the 3'V31 and 3'Dβ1RSS primers to identify the V31<sup>R</sup> allele. To genotype V2<sup>R</sup>/Eβ<sup>Δ</sup> or V31<sup>R</sup>/Eβ<sup>Δ</sup> mice, we performed PCR for the V2<sup>R</sup> or V31<sup>R</sup> allele and Eβ<sup>Δ</sup> allele as described previously (Leduc et al., 2000).

### Flow cytometry

Single-cell suspensions were prepared from the thymuses and spleens of mice and depleted of red blood cells, and Fc receptors were blocked using anti-CD16/CD32. All antibody stains were performed in PBS containing 3% FCS and 0.1% NaN<sub>3</sub> (see Table S3 for a list of all antibodies). To determine effects on gross αβ

T cell development, thymocytes were stained with anti-CD4, anti-CD8α, anti-TCRβ, anti-c-Kit, anti-CD25, and a lineage (Lin) panel composed of anti-TCRγδ, CD11b, CD11c, CD19, B220, TER119, and NK1.1 antibodies. Differential expression of c-Kit and CD25 in Lin<sup>-</sup>CD4<sup>-</sup>CD8<sup>-</sup>TCRβ<sup>-</sup> cells identifies DN1-4 thymocytes. Gross thymocyte development was assessed based on the expression of CD4 and CD8. Peripheral αβ T cell numbers were determined by staining splenocytes with anti-CD4, anti-CD8α, and anti-TCRβ antibodies and identifying CD4<sup>+</sup>TCRβ<sup>+</sup> or CD8<sup>+</sup>TCRβ<sup>+</sup> cells. To monitor Tcrb allelic exclusion, we wished to avoid potential background staining artifacts that can result as a consequence of using biotinylated primary antibodies and streptavidin secondaries. Thus, we ordered directly conjugated anti-Vβ antibodies, most of which are available in only FITC and PE. We stained cells in PBS containing 3% FCS and 0.1% NaN<sub>3</sub> with the following antibodies: anti-CD4 APC-eFluor780, anti-CD8α Pacific Blue, and anti-TCRβ APC. In addition to the aforementioned antibodies, we stained cells with anti-Vβ4 (V2) PE or anti-Vβ14 (V31) FITC, and a corresponding antibody in either FITC or PE, respectively. These are anti-Vβ10<sup>b</sup> (V4) PE, anti-Vβ5.1, 5.2 (V12) FITC or PE, anti-Vβ6 (V19) FITC or PE, and anti-Vβ8 (V13) FITC or PE. Surface TCRβ expression was assayed on singlet and SP (CD4<sup>+</sup> and CD8<sup>+</sup>) cells. Data were collected on an LSR Fortessa and analyzed with FlowJo software (Tree Star). Single cells were gated on the basis of forward and side scatter.

### Generating and analyzing αβ T cell hybridomas

We generated a panel of αβ T cell hybridoma clones using two independent splenocyte cultures from two different V2<sup>R/+</sup>/V31<sup>R/+</sup>

mice, using established methods and reagents (Sleckman et al., 1997). We characterized *Tcrb* rearrangements of each clone by Southern blot analyses using strategies and probes previously described (Bassing et al., 2000, 2008; Khor and Sleckman, 2005; Wu et al., 2003). The *V31<sup>R</sup>* allele contains an additional 101-bp sequence that distinguishes it from an unmodified *V31* allele, and using primers 5′*V31* and 3′*V31* permits us to determine in clones with *V31* rearrangements which *V31* rearranged (Horowitz and Bassing, 2014; Wu et al., 2003). We used the 5′*V2* and 3′*Dβ1RSSRev* primers to PCR-identify which *V2* rearranged in clones with *V2* rearrangements. For clones with recombination of the RSS-replaced *V2* and *V31* segments, we PCR-sequenced each rearrangement using the 5′*V2* or 5′*V31* primer in combination with each of the *Jβ* reverse primers and PCR conditions previously reported (Wu et al., 2003; see Table S2 for a list of all primers).

### Cell sorting

Single-cell suspensions of total thymocytes were stained and sorted to isolate DN1/2 and DN3 thymocytes. Following red blood cell depletion, thymocytes were stained with anti-CD4, anti-CD8α, anti-TCRβ, anti-c-Kit, anti-CD25, and the Lin panel. Thymocytes were first gated on Lin<sup>−</sup>CD4<sup>−</sup>CD8<sup>−</sup>TCRβ<sup>−</sup> cells and then sorted c-Kit<sup>+</sup> cells to isolate DN1/2 cells or c-Kit<sup>−</sup>CD25<sup>+</sup> cells to isolate DN3 cells.

### Real-time quantitative PCR (qPCR) analysis

TaqMan qPCR assays were performed on DNA isolated from sorted DN1/2 and DN3 thymocytes to detect *Vβ(Dβ1)Jβ1.1*, *Vβ(Dβ)Jβ2.1*, and *Dβ2Jβ2.1* rearrangements using previously described reagents and methods (Gopalakrishnan et al., 2013). Total *VβDβJβ1.1*, *VβDβJβ2.1*, and *Dβ2Jβ2.1* rearrangements were normalized to an unrearranged region of the genome (*CD19*).

### Quantification and statistical analysis

Data are reported as mean ± SD. Statistical analyses were done with Prism 8.

### Online supplemental material

Fig. S1 provides sequence validation for the *V2* and *V31* RSS replacements. Fig. S2 provides analysis of thymocyte and αβ T cell development. Fig. S3 provides analysis of *V2* and *V31* rearrangements in DN thymocytes. Fig. S4 shows similar changes in the *Vβ* repertoire of RSS replacement mice in peripheral αβ T cells. Fig. S5 shows peripheral αβ T cells with biallelic *Tcrb* gene expression. Table S1 provides analysis of *Tcrb* rearrangements in *Tcrb<sup>Tg</sup>* hybridomas. Table S2 is a list of oligonucleotides used to generate, genotype, and sequence the mouse models as well as to perform the TaqMan qPCR. Table S3 is a list of all the key reagents to perform flow cytometry and create hybridomas, and additional mouse strains used.

### Acknowledgments

We thank Adele Harman and Jennifer Dunlap of the CHOP Transgenics Core for help establishing all *Vβ* RSS replacement mice and the CHOP Flow Cytometry Core for assistance with

analytic analyses and cell sorting. We thank Drs. Grace Teng, Yuhang Zhang, David G. Schatz, and Gene Oltz for helpful discussions of this research and the manuscript.

National Institutes of Health grants T32 AI055428 (G.S. Wu) and RO1 AI 130231 (C.H. Bassing) supported this work.

Author contributions: C.H. Bassing conceived and supervised this study. C.H. Bassing and K.S. Yang-Iott designed the *V2<sup>R</sup>* and *V31<sup>R</sup>* modifications. G.S. Wu designed the *V2<sup>F</sup>* and *V31<sup>F</sup>* modifications. G.S. Wu and C.H. Bassing designed the research plan. G.S. Wu, with assistance from K.D. Lee, conducted and analyzed all mouse experiments. K.S. Yang-Iott and M.A. Klink made and analyzed hybridomas, and worked with G.S. Wu and C.H. Bassing to identify *Tcrb* rearrangements. K.E. Hayer performed all statistical analyses. G.S. Wu and C.H. Bassing worked together to prepare the manuscript.

Disclosures: The authors declare no competing interests exist.

Submitted: 4 March 2020

Revised: 6 May 2020

Accepted: 12 May 2020

### References

- Agata, Y., N. Tamaki, S. Sakamoto, T. Ikawa, K. Masuda, H. Kawamoto, and C. Murte. 2007. Regulation of T cell receptor beta gene rearrangements and allelic exclusion by the helix-loop-helix protein, E47. *Immunity*. 27: 871–884. <https://doi.org/10.1016/j.immuni.2007.11.015>
- Akira, S., K. Okazaki, and H. Sakano. 1987. Two pairs of recombination signals are sufficient to cause immunoglobulin V-(D)-J joining. *Science*. 238: 1134–1138. <https://doi.org/10.1126/science.3120312>
- Banerjee, J.K., and D.G. Schatz. 2014. Synapsis alters RAG-mediated nicking at *Tcrb* recombination signal sequences: implications for the “beyond 12/23” rule. *Mol. Cell. Biol.* 34:2566–2580. <https://doi.org/10.1128/MCB.00411-14>
- Bassing, C.H., F.W. Alt, M.M. Hughes, M. D’Auteuil, T.D. Wehrly, B.B. Woodman, F. Gärtner, J.M. White, L. Davidson, and B.P. Sleckman. 2000. Recombination signal sequences restrict chromosomal V(D)J recombination beyond the 12/23 rule. *Nature*. 405:583–586. <https://doi.org/10.1038/35014635>
- Bassing, C.H., W. Swat, and F.W. Alt. 2002. The mechanism and regulation of chromosomal V(D)J recombination. *Cell*. 109(2, Suppl):S45–S55. [https://doi.org/10.1016/S0092-8674\(02\)00675-X](https://doi.org/10.1016/S0092-8674(02)00675-X)
- Bassing, C.H., S. Whitlow, R. Mostoslavsky, K. Yang-Iott, S. Ranganath, and F.W. Alt. 2008. Vbeta cluster sequences reduce the frequency of primary Vbeta2 and Vbeta14 rearrangements. *Eur. J. Immunol.* 38:2564–2572. <https://doi.org/10.1002/eji.200838347>
- Bolland, D.J., H. Koohy, A.L. Wood, L.S. Matheson, F. Krueger, M.J. Stubbington, A. Baizan-Edge, P. Chovanec, B.A. Stubbs, K. Tabbada, et al. 2016. Two Mutually Exclusive Local Chromatin States Drive Efficient V(D)J Recombination. *Cell Rep.* 15:2475–2487. <https://doi.org/10.1016/j.celrep.2016.05.020>
- Bories, J.C., J. Demengeot, L. Davidson, and F.W. Alt. 1996. Gene-targeted deletion and replacement mutations of the T-cell receptor beta-chain enhancer: the role of enhancer elements in controlling V(D)J recombination accessibility. *Proc. Natl. Acad. Sci. USA*. 93:7871–7876. <https://doi.org/10.1073/pnas.93.15.7871>
- Bouvier, G., F. Watrin, M. Naspetti, C. Verthuy, P. Naquet, and P. Ferrier. 1996. Deletion of the mouse T-cell receptor beta gene enhancer blocks alphabeta T-cell development. *Proc. Natl. Acad. Sci. USA*. 93:7877–7881. <https://doi.org/10.1073/pnas.93.15.7877>
- Brady, B.L., N.C. Steinel, and C.H. Bassing. 2010. Antigen receptor allelic exclusion: an update and reappraisal. *J. Immunol.* 185:3801–3808. <https://doi.org/10.4049/jimmunol.1001158>
- Chan, E.A., G. Teng, E. Corbett, K.R. Choudhury, C.H. Bassing, D.G. Schatz, and M.S. Krangel. 2013. Peripheral subnuclear positioning suppresses *Tcrb* recombination and segregates *Tcrb* alleles from

- RAG2. *Proc. Natl. Acad. Sci. USA.* 110:E4628–E4637. <https://doi.org/10.1073/pnas.1310846110>
- Chen, S., B. Lee, A.Y. Lee, A.J. Modzelewski, and L. He. 2016. Highly Efficient Mouse Genome Editing by CRISPR Ribonucleoprotein Electroporation of Zygotes. *J. Biol. Chem.* 291:14457–14467. <https://doi.org/10.1074/jbc.M116.733154>
- Chen, S., T.R. Luperchio, X. Wong, E.B. Doan, A.T. Byrd, K. Roy Choudhury, K.L. Reddy, and M.S. Krangel. 2018. A Lamina-Associated Domain Border Governs Nuclear Lamina Interactions, Transcription, and Recombination of the Tcrb Locus. *Cell Rep.* 25:1729–1740.e6. <https://doi.org/10.1016/j.celrep.2018.10.052>
- Connor, A.M., L.J. Fanning, J.W. Celler, L.K. Hicks, D.A. Ramsden, and G.E. Wu. 1995. Mouse VH7183 recombination signal sequences mediate recombination more frequently than those of VHJ558. *J. Immunol.* 155: 5268–5272.
- Cowell, L.G., M. Davila, K. Yang, T.B. Kepler, and G. Kelsoe. 2003. Prospective estimation of recombination signal efficiency and identification of functional cryptic signals in the genome by statistical modeling. *J. Exp. Med.* 197:207–220. <https://doi.org/10.1084/jem.20020250>
- Drejer-Teel, A.H., S.D. Fugmann, and D.G. Schatz. 2007. The beyond 12/23 restriction is imposed at the nicking and pairing steps of DNA cleavage during V(D)J recombination. *Mol. Cell Biol.* 27:6288–6299. <https://doi.org/10.1128/MCB.00835-07>
- Farago, M., C. Rosenbluh, M. Tevlin, S. Fraenkel, S. Schlesinger, H. Masika, M. Gouzman, G. Teng, D. Schatz, Y. Rais, et al. 2012. Clonal allelic predetermination of immunoglobulin- $\kappa$  rearrangement. *Nature.* 490: 561–565. <https://doi.org/10.1038/nature11496>
- Fisher, M.R., A. Rivera-Reyes, N.B. Bloch, D.G. Schatz, and C.H. Bassing. 2017. Immature Lymphocytes Inhibit *Rag1* and *Rag2* Transcription and V(D)J Recombination in Response to DNA Double-Strand Breaks. *J. Immunol.* 198:2943–2956. <https://doi.org/10.4049/jimmunol.1601639>
- Fuxa, M., J. Skok, A. Souabni, G. Salvaggio, E. Roldan, and M. Busslinger. 2004. Pax5 induces V-to-DJ rearrangements and locus contraction of the immunoglobulin heavy-chain gene. *Genes Dev.* 18:411–422. <https://doi.org/10.1101/gad.291504>
- Gauss, G.H., and M.R. Lieber. 1992. The basis for the mechanistic bias for deletional over inversional V(D)J recombination. *Genes Dev.* 6:1553–1561. <https://doi.org/10.1101/gad.6.8.1553>
- Godfrey, D.I., J. Kennedy, T. Suda, and A. Zlotnik. 1993. A developmental pathway involving four phenotypically and functionally distinct subsets of CD3-CD4-CD8- triple-negative adult mouse thymocytes defined by CD44 and CD25 expression. *J. Immunol.* 150:4244–4252.
- Gopalakrishnan, S., K. Majumder, A. Predeus, Y. Huang, O.I. Koues, J. Verma-Gaur, S. Loguercio, A.I. Su, A.J. Feeney, M.N. Artyomov, et al. 2013. Unifying model for molecular determinants of the preselection V $\beta$  repertoire. *Proc. Natl. Acad. Sci. USA.* 110:E3206–E3215. <https://doi.org/10.1073/pnas.1304048110>
- Hesse, J.E., M.R. Lieber, K. Mizuuchi, and M. Gellert. 1989. V(D)J recombination: a functional definition of the joining signals. *Genes Dev.* 3: 1053–1061. <https://doi.org/10.1101/gad.3.7.1053>
- Hewitt, S.L., B. Yin, Y. Ji, J. Chaumeil, K. Marszalek, J. Tenthorey, G. Salvaggio, N. Steinel, L.B. Ramsey, J. Ghysdael, et al. 2009. RAG-1 and ATM coordinate monoallelic recombination and nuclear positioning of immunoglobulin loci. *Nat. Immunol.* 10:655–664. <https://doi.org/10.1038/ni.1735>
- Horowitz, J.E., and C.H. Bassing. 2014. Noncore RAG1 regions promote V $\beta$  rearrangements and  $\alpha\beta$  T cell development by overcoming inherent inefficiency of V $\beta$  recombination signal sequences. *J. Immunol.* 192: 1609–1619. <https://doi.org/10.4049/jimmunol.1301599>
- Jackson, A.M., and M.S. Krangel. 2005. Allele-specific regulation of TCR beta variable gene segment chromatin structure. *J. Immunol.* 175:5186–5191. <https://doi.org/10.4049/jimmunol.175.8.5186>
- Jain, S., Z. Ba, Y. Zhang, H.Q. Dai, and F.W. Alt. 2018. CTCF-Binding Elements Mediate Accessibility of RAG Substrates During Chromatin Scanning. *Cell.* 174:102–116.e14. <https://doi.org/10.1016/j.cell.2018.04.035>
- Ji, Y., A.J. Little, J.K. Banerjee, B. Hao, E.M. Oltz, M.S. Krangel, and D.G. Schatz. 2010. Promoters, enhancers, and transcription target RAG1 binding during V(D)J recombination. *J. Exp. Med.* 207:2809–2816. <https://doi.org/10.1084/jem.20101136>
- Jung, D., C.H. Bassing, S.D. Fugmann, H.L. Cheng, D.G. Schatz, and F.W. Alt. 2003. Extrachromosomal recombination substrates recapitulate beyond 12/23 restricted VDJ recombination in nonlymphoid cells. *Immunity.* 18:65–74. [https://doi.org/10.1016/S1074-7613\(02\)00507-1](https://doi.org/10.1016/S1074-7613(02)00507-1)
- Khamlichi, A.A., and R. Feil. 2018. Parallels between Mammalian Mechanisms of Monoallelic Gene Expression. *Trends Genet.* 34:954–971. <https://doi.org/10.1016/j.tig.2018.08.005>
- Khor, B., and B.P. Sleckman. 2005. Intra- and inter-allelic ordering of T cell receptor beta chain gene assembly. *Eur. J. Immunol.* 35:964–970. <https://doi.org/10.1002/eji.200425806>
- Kim, M.S., W. Chuenchor, X. Chen, Y. Cui, X. Zhang, Z.H. Zhou, M. Gellert, and W. Yang. 2018. Cracking the DNA Code for V(D)J Recombination. *Mol. Cell.* 70:358–370.e4. <https://doi.org/10.1016/j.molcel.2018.03.008>
- Larijani, M., C.C. Yu, R. Golub, Q.L. Lam, and G.E. Wu. 1999. The role of components of recombination signal sequences in immunoglobulin gene segment usage: a V81x model. *Nucleic Acids Res.* 27:2304–2309. <https://doi.org/10.1093/nar/27.11.2304>
- Leduc, I., W.M. Hempel, N. Mathieu, C. Verthuy, G. Bouvier, F. Watrin, and P. Ferrier. 2000. T cell development in TCR beta enhancer-deleted mice: implications for alpha beta T cell lineage commitment and differentiation. *J. Immunol.* 165:1364–1373. <https://doi.org/10.4049/jimmunol.165.3.1364>
- Levin-Klein, R., and Y. Bergman. 2014. Epigenetic regulation of monoallelic rearrangement (allelic exclusion) of antigen receptor genes. *Front. Immunol.* 5:625. <https://doi.org/10.3389/fimmu.2014.00625>
- Liang, H.E., L.Y. Hsu, D. Cado, L.G. Cowell, G. Kelsoe, and M.S. Schlissel. 2002. The “dispensable” portion of RAG2 is necessary for efficient V-to-DJ rearrangement during B and T cell development. *Immunity.* 17: 639–651. [https://doi.org/10.1016/S1074-7613\(02\)00448-X](https://doi.org/10.1016/S1074-7613(02)00448-X)
- Lin, W.C., and S. Desiderio. 1994. Cell cycle regulation of V(D)J recombination-activating protein RAG-2. *Proc. Natl. Acad. Sci. USA.* 91:2733–2737. <https://doi.org/10.1073/pnas.91.7.2733>
- Livak, F., D.B. Burtrum, L. Rowen, D.G. Schatz, and H.T. Petrie. 2000. Genetic modulation of T cell receptor gene segment usage during somatic recombination. *J. Exp. Med.* 192:1191–1196. <https://doi.org/10.1084/jem.192.8.1191>
- Lovely, G.A., R.C. Brewster, D.G. Schatz, D. Baltimore, and R. Phillips. 2015. Single-molecule analysis of RAG-mediated V(D)J DNA cleavage. *Proc. Natl. Acad. Sci. USA.* 112:E1715–E1723. <https://doi.org/10.1073/pnas.1503477112>
- Majumder, K., O.I. Koues, E.A. Chan, K.E. Kyle, J.E. Horowitz, K. Yang-Iott, C.H. Bassing, I. Taniuchi, M.S. Krangel, and E.M. Oltz. 2015. Lineage-specific compaction of Tcrb requires a chromatin barrier to protect the function of a long-range tethering element. *J. Exp. Med.* 212:107–120. <https://doi.org/10.1084/jem.20141479>
- Malissen, M., C. McCoy, D. Blanc, J. Trucy, C. Devaux, A.M. Schmitt-Verhulst, F. Fitch, L. Hood, and B. Malissen. 1986. Direct evidence for chromosomal inversion during T-cell receptor beta-gene rearrangements. *Nature.* 319:28–33. <https://doi.org/10.1038/319028a0>
- Mostoslavsky, R., N. Singh, T. Tenzen, M. Goldmit, C. Gabay, S. Elizur, P. Qi, B.E. Reubinoff, A. Chess, H. Cedar, et al. 2001. Asynchronous replication and allelic exclusion in the immune system. *Nature.* 414:221–225. <https://doi.org/10.1038/35102606>
- Mostoslavsky, R., F.W. Alt, and K. Rajewsky. 2004. The lingering enigma of the allelic exclusion mechanism. *Cell.* 118:539–544. <https://doi.org/10.1016/j.cell.2004.08.023>
- Nadel, B., A. Tang, G. Escuro, G. Lugo, and A.J. Feeney. 1998. Sequence of the spacer in the recombination signal sequence affects V(D)J rearrangement frequency and correlates with nonrandom V $\kappa$  usage in vivo. *J. Exp. Med.* 187:1495–1503. <https://doi.org/10.1084/jem.187.9.1495>
- Olaru, A., D.N. Patterson, H. Cai, and F. Livák. 2004. Recombination signal sequence variations and the mechanism of patterned T-cell receptor-beta locus rearrangement. *Mol. Immunol.* 40:1189–1201. <https://doi.org/10.1016/j.molimm.2003.11.019>
- Outters, P., S. Jaeger, N. Zaarour, and P. Ferrier. 2015. Long-Range Control of V(D)J Recombination & Allelic Exclusion: Modeling Views. *Adv. Immunol.* 128:363–413. <https://doi.org/10.1016/bs.ai.2015.08.002>
- Powers, S.E., M. Mandal, S. Matsuda, A.V. Miletic, M.H. Cato, A. Tanaka, R.C. Rickert, S. Koyasu, and M.R. Clark. 2012. Subnuclear cyclin D3 compartments and the coordinated regulation of proliferation and immunoglobulin variable gene repression. *J. Exp. Med.* 209:2199–2213. <https://doi.org/10.1084/jem.20120800>
- Ramsden, D.A., and G.E. Wu. 1991. Mouse kappa light-chain recombination signal sequences mediate recombination more frequently than do those of lambda light chain. *Proc. Natl. Acad. Sci. USA.* 88:10721–10725. <https://doi.org/10.1073/pnas.88.23.10721>
- Ran, F.A., P.D. Hsu, J. Wright, V. Agarwala, D.A. Scott, and F. Zhang. 2013. Genome engineering using the CRISPR-Cas9 system. *Nat. Protoc.* 8: 2281–2308. <https://doi.org/10.1038/nprot.2013.143>
- Ru, H., M.G. Chambers, T.M. Fu, A.B. Tong, M. Liao, and H. Wu. 2015. Molecular Mechanism of V(D)J Recombination from Synaptic RAG1-RAG2 Complex Structures. *Cell.* 163:1138–1152. <https://doi.org/10.1016/j.cell.2015.10.055>

- Ryu, C.J., B.B. Haines, H.R. Lee, Y.H. Kang, D.D. Draganov, M. Lee, C.E. Whitehurst, H.J. Hong, and J. Chen. 2004. The T-cell receptor beta variable gene promoter is required for efficient V beta rearrangement but not allelic exclusion. *Mol. Cell. Biol.* 24:7015-7023. <https://doi.org/10.1128/MCB.24.16.7015-7023.2004>
- Schatz, D.G., and P.C. Swanson. 2011. V(D)J recombination: mechanisms of initiation. *Annu. Rev. Genet.* 45:167-202. <https://doi.org/10.1146/annurev-genet-110410-132552>
- Schlimgen, R.J., K.L. Reddy, H. Singh, and M.S. Krangel. 2008. Initiation of allelic exclusion by stochastic interaction of Tcrb alleles with repressive nuclear compartments. *Nat. Immunol.* 9:802-809. <https://doi.org/10.1038/ni.1624>
- Shih, H.Y., and M.S. Krangel. 2013. Chromatin architecture, CCCTC-binding factor, and V(D)J recombination: managing long-distance relationships at antigen receptor loci. *J. Immunol.* 190:4915-4921. <https://doi.org/10.4049/jimmunol.1300218>
- Shinkai, Y., S. Koyasu, K. Nakayama, K.M. Murphy, D.Y. Loh, E.L. Reinherz, and F.W. Alt. 1993. Restoration of T cell development in RAG-2-deficient mice by functional TCR transgenes. *Science*. 259:822-825. <https://doi.org/10.1126/science.8430336>
- Sicinska, E., I. Aifantis, L. Le Cam, W. Swat, C. Borowski, Q. Yu, A.A. Ferrando, S.D. Levin, Y. Geng, H. von Boehmer, et al. 2003. Requirement for cyclin D3 in lymphocyte development and T cell leukemias. *Cancer Cell*. 4:451-461. [https://doi.org/10.1016/S1535-6108\(03\)00301-5](https://doi.org/10.1016/S1535-6108(03)00301-5)
- Skok, J.A., R. Gisler, M. Novatchkova, D. Farmer, W. de Laat, and M. Buslinger. 2007. Reversible contraction by looping of the Tcra and Tcrb loci in rearranging thymocytes. *Nat. Immunol.* 8:378-387. <https://doi.org/10.1038/ni1448>
- Sleckman, B.P., C.G. Bardon, R. Ferrini, L. Davidson, and F.W. Alt. 1997. Function of the TCR alpha enhancer in alphabeta and gammadelta T cells. *Immunity*. 7:505-515. [https://doi.org/10.1016/S1074-7613\(00\)80372-6](https://doi.org/10.1016/S1074-7613(00)80372-6)
- Sleckman, B.P., C.H. Bassing, M.M. Hughes, A. Okada, M. D'Auteuil, T.D. Wehrly, B.B. Woodman, L. Davidson, J. Chen, and F.W. Alt. 2000. Mechanisms that direct ordered assembly of T cell receptor beta locus V, D, and J gene segments. *Proc. Natl. Acad. Sci. USA*. 97:7975-7980. <https://doi.org/10.1073/pnas.130190597>
- Steinel, N.C., B.L. Brady, A.C. Carpenter, K.S. Yang-Iott, and C.H. Bassing. 2010. Posttranscriptional silencing of VbetaDJbetaCbeta genes contributes to TCRbeta allelic exclusion in mammalian lymphocytes. *J. Immunol.* 185:1055-1062. <https://doi.org/10.4049/jimmunol.0903099>
- Steinel, N.C., B.S. Lee, A.T. Tubbs, J.J. Bednarski, E. Schulte, K.S. Yang-Iott, D.G. Schatz, B.P. Sleckman, and C.H. Bassing. 2013. The ataxia telangiectasia mutated kinase controls I $\kappa$  allelic exclusion by inhibiting secondary V $\kappa$ -to-J $\kappa$  rearrangements. *J. Exp. Med.* 210:233-239. <https://doi.org/10.1084/jem.20121605>
- Tillman, R.E., A.L. Wooley, B. Khor, T.D. Wehrly, C.A. Little, and B.P. Sleckman. 2003. Cutting edge: targeting of V beta to D beta rearrangement by RSSs can be mediated by the V(D)J recombinase in the absence of additional lymphoid-specific factors. *J. Immunol.* 170:5-9. <https://doi.org/10.4049/jimmunol.170.1.5>
- VanDyk, L.F., T.W. Wise, B.B. Moore, and K. Meek. 1996. Immunoglobulin D(H) recombination signal sequence targeting: effect of D(H) coding and flanking regions and recombination partner. *J. Immunol.* 157:4005-4015.
- Vettermann, C., and M.S. Schlissel. 2010. Allelic exclusion of immunoglobulin genes: models and mechanisms. *Immunol. Rev.* 237:22-42. <https://doi.org/10.1111/j.1600-065X.2010.00935.x>
- Wang, X., G. Xiao, Y. Zhang, X. Wen, X. Gao, S. Okada, and X. Liu. 2008. Regulation of Tcrb recombination ordering by c-Fos-dependent RAG deposition. *Nat. Immunol.* 9:794-801. <https://doi.org/10.1038/ni.1614>
- Wang, H., H. Yang, C.S. Shivalila, M.M. Dawlaty, A.W. Cheng, F. Zhang, and R. Jaenisch. 2013. One-step generation of mice carrying mutations in multiple genes by CRISPR/Cas-mediated genome engineering. *Cell*. 153:910-918. <https://doi.org/10.1016/j.cell.2013.04.025>
- Wei, Z., and M.R. Lieber. 1993. Lymphoid V(D)J recombination. Functional analysis of the spacer sequence within the recombination signal. *J. Biol. Chem.* 268:3180-3183.
- Wilson, A., C. Maréchal, and H.R. MacDonald. 2001. Biased V beta usage in immature thymocytes is independent of DJ beta proximity and pT alpha pairing. *J. Immunol.* 166:51-57. <https://doi.org/10.4049/jimmunol.166.1.51>
- Wu, C., C.H. Bassing, D. Jung, B.B. Woodman, D. Foy, and F.W. Alt. 2003. Dramatically increased rearrangement and peripheral representation of Vbeta14 driven by the 3'Dbeta14 recombination signal sequence. *Immunity*. 18:75-85. [https://doi.org/10.1016/S1074-7613\(02\)00515-0](https://doi.org/10.1016/S1074-7613(02)00515-0)
- Wu, C., S. Ranganath, M. Gleason, B.B. Woodman, T.M. Borjeson, F.W. Alt, and C.H. Bassing. 2007. Restriction of endogenous T cell antigen receptor beta rearrangements to Vbeta14 through selective recombination signal sequence modifications. *Proc. Natl. Acad. Sci. USA*. 104:4002-4007. <https://doi.org/10.1073/pnas.0700081104>
- Yang-Iott, K.S., A.C. Carpenter, M.A. Rowh, N. Steinel, B.L. Brady, K. Hochedlinger, R. Jaenisch, and C.H. Bassing. 2010. TCR beta feedback signals inhibit the coupling of recombinationally accessible V beta 14 segments with DJ beta complexes. *J. Immunol.* 184:1369-1378. <https://doi.org/10.4049/jimmunol.0900723>

## Supplemental material

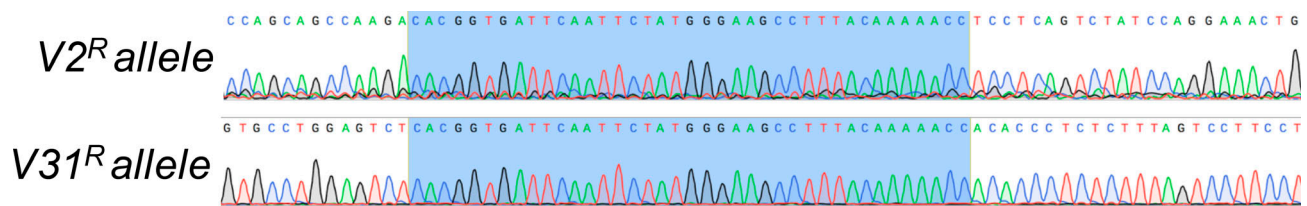


Figure S1. **Validation of V2 and V31 RSS replacement mice.** Sequence validation of the V2 or V31 RSS replacement with the 3'Dβ1 RSS. The 3'Dβ1 RSSs are highlighted in blue.

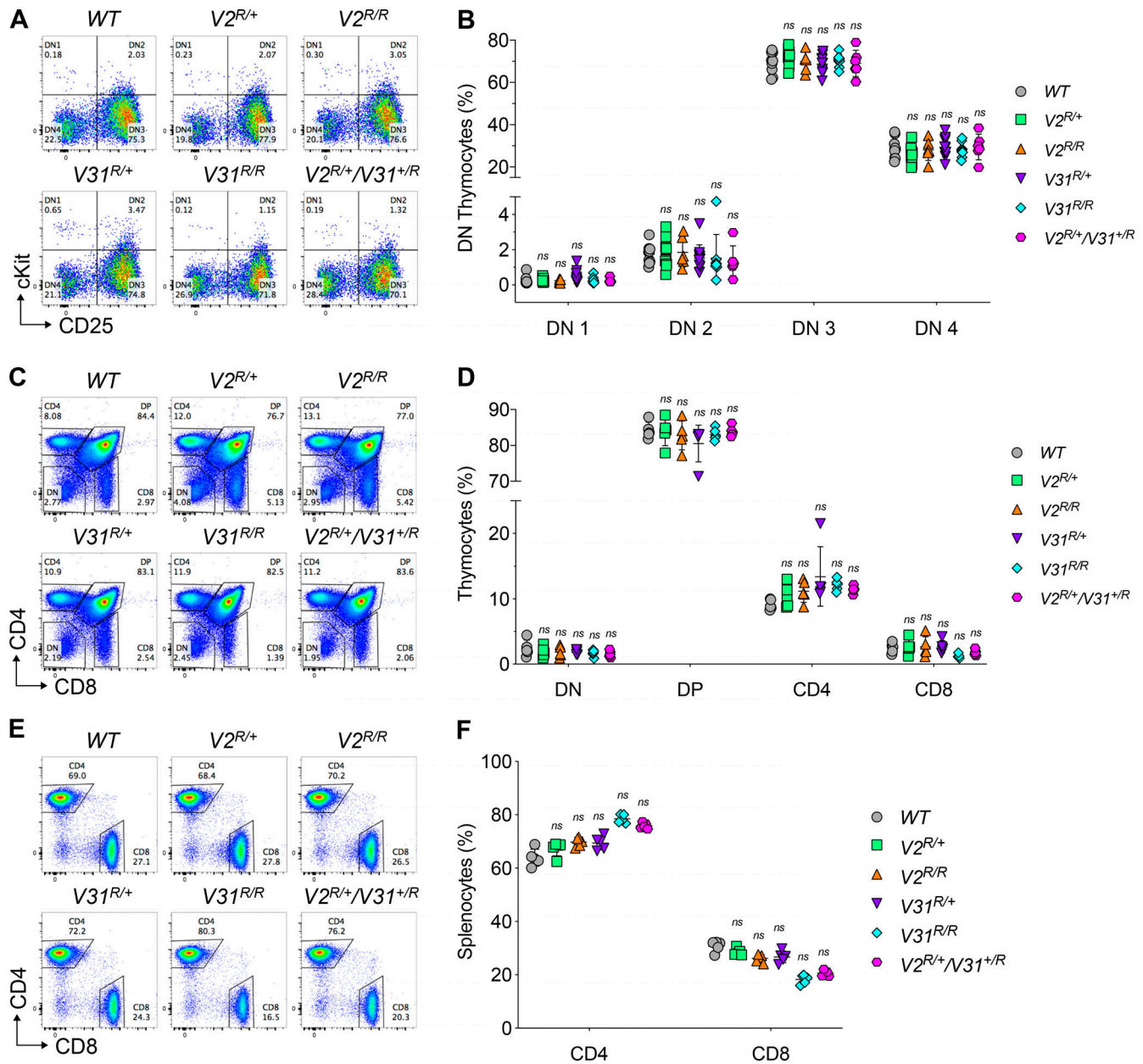


Figure S2. **Normal gross  $\alpha\beta$  T cell development in V2 and V31 RSS replacement mice.** (A and B) DN thymocyte development. Representative plots (A) and quantification (B) of DN cells. Gated on Lin<sup>-</sup>CD4<sup>-</sup>CD8<sup>-</sup>TCR $\beta$ <sup>-</sup> thymocytes ( $n \geq 5$  mice per group). (C and D) Global thymocyte development. Representative plots (C) and quantification (D) of DN, DP, CD4<sup>+</sup>, and CD8<sup>+</sup> thymocytes ( $n = 5$  mice per group). (E and F) Representative plots (E) and quantification (F) of SP  $\alpha\beta$  T cells in the spleen. Gated on TCR $\beta$ <sup>+</sup> cells ( $n = 5$  mice per group). (B, D, and F) Two-way ANOVA followed by Dunnett's post-tests for multiple comparisons. All quantification plots show mean  $\pm$  SD. Data in B, D, and F are compiled from at least five experiments.

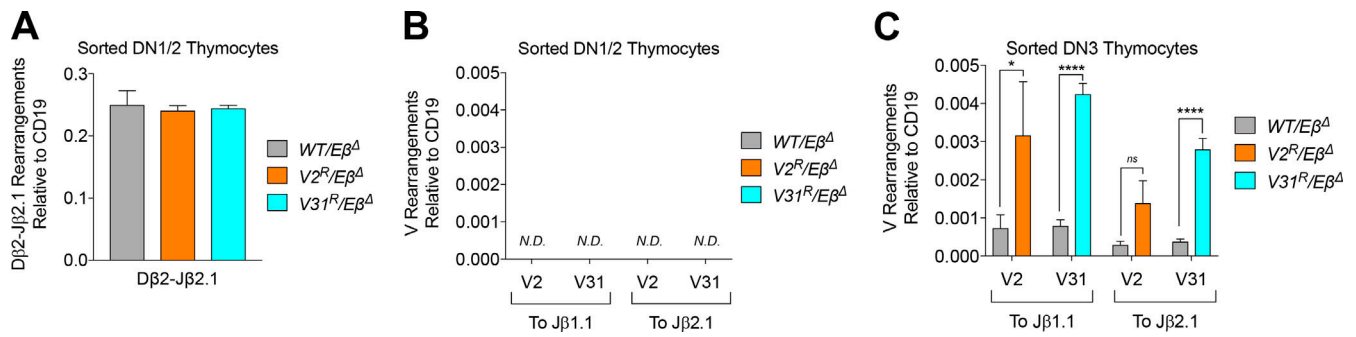


Figure S3. **The 3'Dβ1 RSS replacement increases V2 and V31 recombination in DN3 thymocytes.** (A) Quantification of Dβ2-Jβ2.1 rearrangements by TaqMan qPCR in DN1/2 thymocytes ( $n = 3$  mice per group). (B and C) Quantification of indicated Vβ rearrangements by TaqMan qPCR in DN1/2 (B) or DN3 (C) thymocytes ( $n = 3$  mice per group, two-way ANOVA followed by Bonferroni's post-tests for multiple comparisons). These data are compiled from three experiments. N.D., not determined; \*,  $P < 0.05$ ; \*\*\*\*,  $P < 0.0001$ .

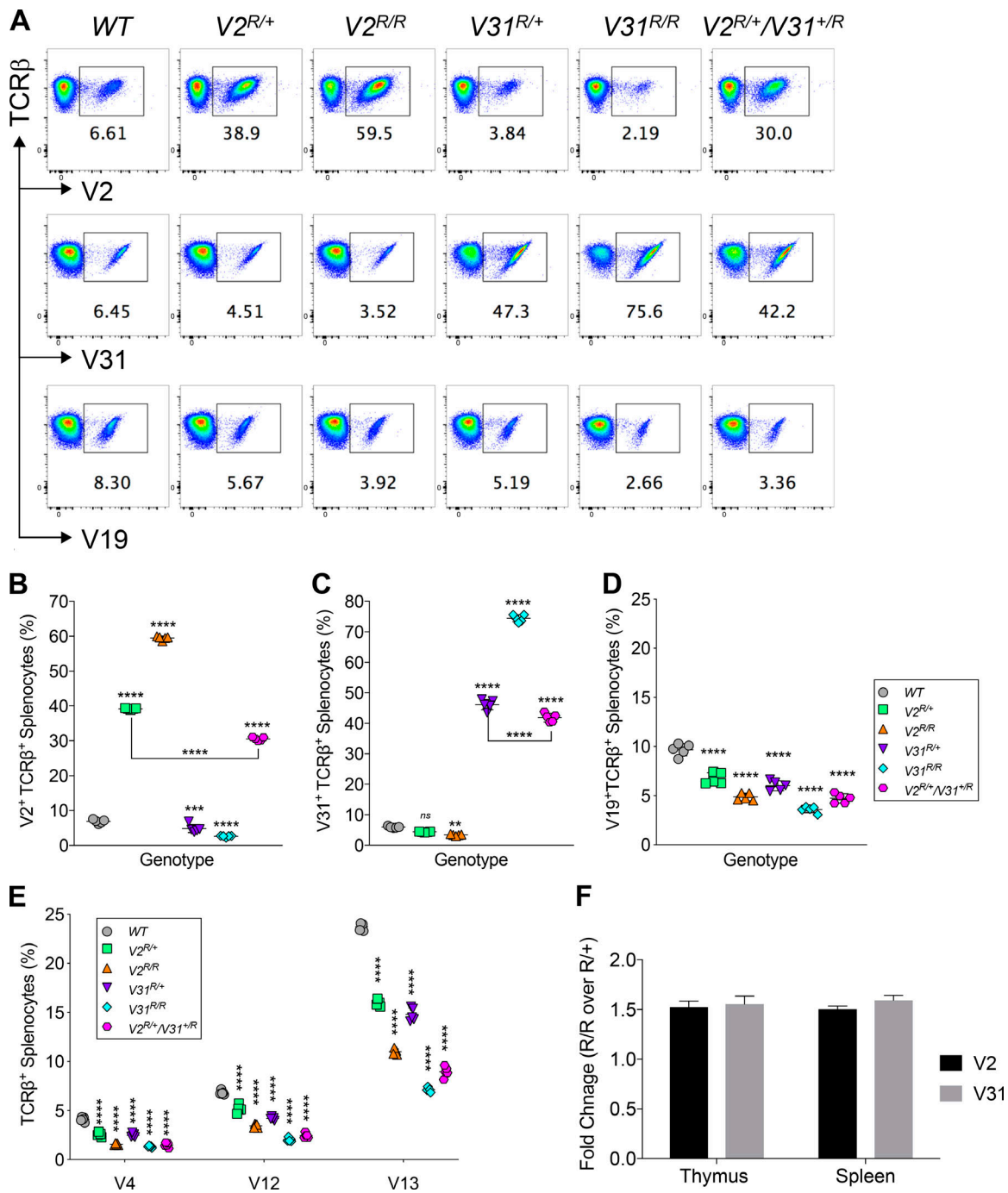


Figure S4. **Peripheral  $\alpha\beta$  T cells exhibit similar shifts in the  $V\beta$  repertoire in RSS replacement mice.** (A) Representative plots of SP splenocytes expressing V2<sup>+</sup>, V31<sup>+</sup>, or V19<sup>+</sup> TCR $\beta$  chains. (B–D) Quantification of V2<sup>+</sup> (B), V31<sup>+</sup> (C), or V19<sup>+</sup> (D) SP thymocytes ( $n = 5$  mice per group, one-way ANOVA followed by Tukey's post-tests for multiple comparisons). (E) Quantification of SP splenocytes expressing V4<sup>+</sup>, V12<sup>+</sup>, or V13<sup>+</sup> TCR $\beta$  chains ( $n = 5$  mice per group, two-way ANOVA followed by Tukey's post-tests for multiple comparisons). (F) Ratio of the V2<sup>+</sup> and V31<sup>+</sup>  $V\beta$  repertoires. The fold change calculates the frequency of V2<sup>+</sup> cells from V2<sup>R/R</sup> mice divided by V2<sup>R/+</sup> mice. A similar calculation was made for V31<sup>+</sup> cells from V31<sup>R/R</sup> and V31<sup>R/+</sup> mice. All quantification plots show mean  $\pm$  SD. Multiple post-tests are compared with WT unless indicated by bars, and P values are corrected for multiple tests. ns, not significant; \*\*,  $P < 0.01$ ; \*\*\*,  $P < 0.001$ ; \*\*\*\*,  $P < 0.0001$ . Data in B–F are compiled from five experiments.

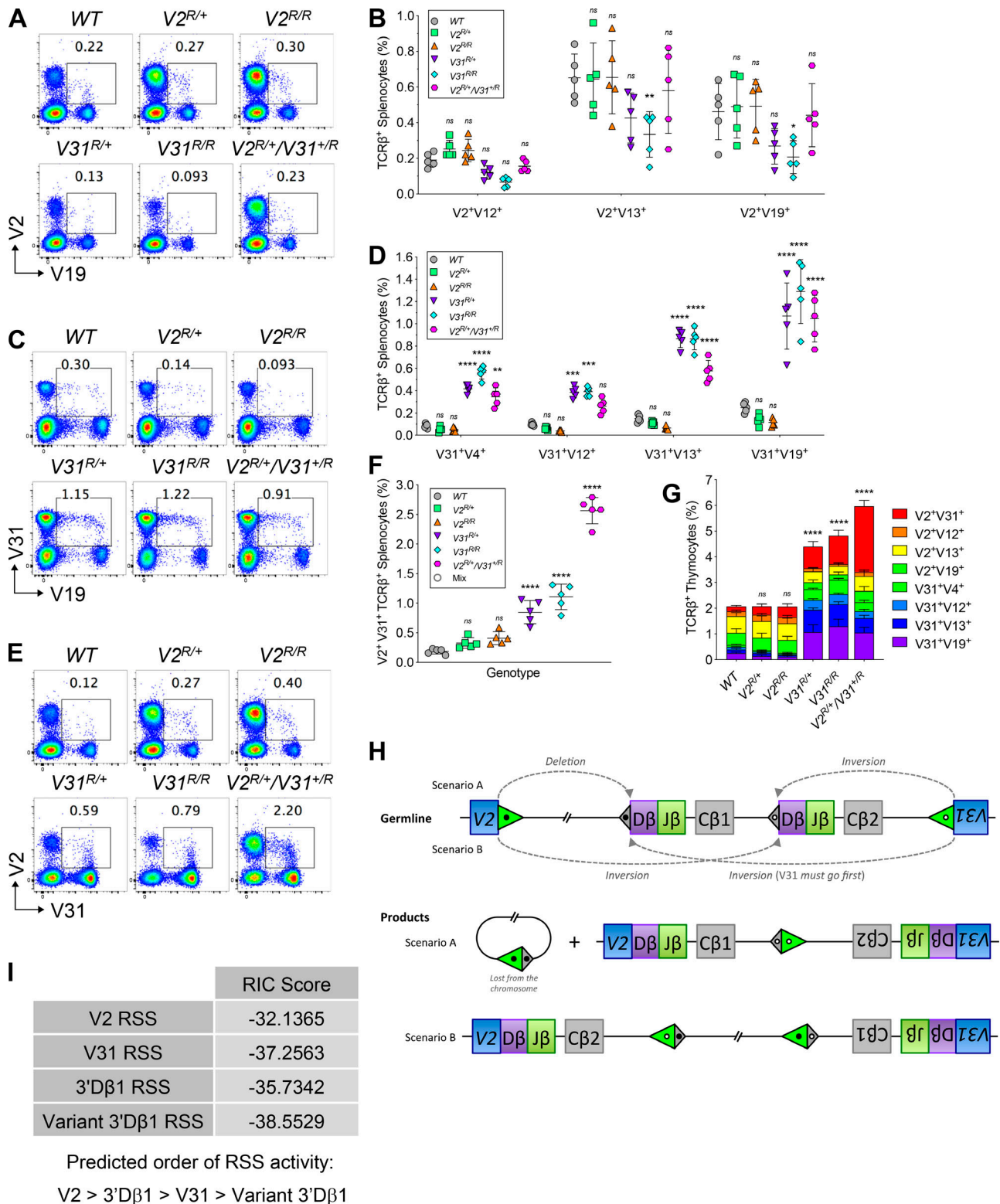


Figure S5.  **$\alpha\beta$  T cells exhibiting biallelic *Tcrb* gene expression seed the periphery.** (A, C, and E) Representative plots of SP splenocytes expressing both V2<sup>+</sup> and V19<sup>+</sup> (A), V31<sup>+</sup> and V19<sup>+</sup> (C), or V2<sup>+</sup> and V31<sup>+</sup> (E) TCRβ chains. (B, D, and F) Quantification of SP splenocytes expressing the two indicated TCRβ chains. *n* = 5 mice per group, two-way ANOVA followed by Tukey's post-tests for multiple comparisons (B and D), one-way ANOVA followed by Dunnett's post-tests comparing each RSS mutant to WT (F). (G) Quantification of double-staining SP splenocytes for each Vβ combination tested (*n* = 5 mice per group, two-way ANOVA). (H) Depiction of the recombination events that could result in two TCRβ chains expressed from one allele. RSSs indicated as triangles. (I) RIC scores of RSSs in this study, generated by RSSSite (<https://www.itb.cnr.it/rss/>). All quantification plots show mean ± SD. Multiple post-tests are compared with WT unless indicated by bars, and P values are corrected for multiple tests. ns, not significant, \*, *P* < 0.05; \*\*, *P* < 0.01; \*\*\*, *P* < 0.001; \*\*\*\*, *P* < 0.0001. Data in B, D, F, and G are compiled from five experiments.

Tables S1–S3 are provided online as separate files. Table S1 is an analysis of *Tcrb* rearrangements in *Tcrb*<sup>Tg</sup> T cell hybridomas. Table S2 shows oligonucleotides used for generating mouse lines, genotyping, sequencing, and TaqMan qPCR. Table S3 shows key reagents.